e-ISSN: 3023-6487

JRM

Journal of Radiology in Medicine

Volume: 1

Issue: 4

Year: 2024

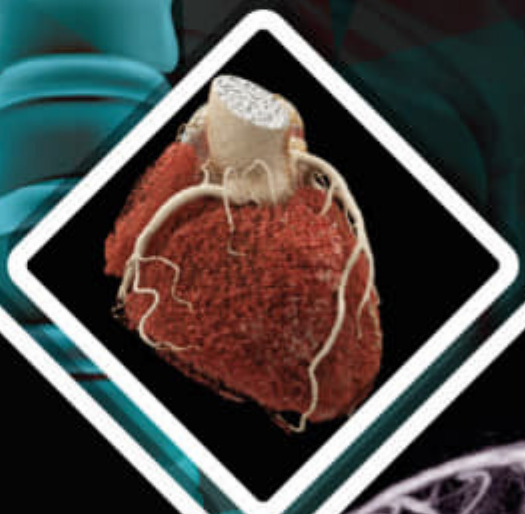

MHA
MEDIHEALTH ACADEMY

EDITORS-IN-CHIEF

EDITORIAL BOARD

ENGLISH LANGUAGE EDITOR

Assoc. Prof. Mehmet ZENGİN

Department of Pathology, Ankara Training and Resarch Hospital, University of Health Sciences, Ankara, Turkiye

STATISTICS EDITOR

Assist. Prof. Emrah DOĞAN

Department of Radiology, Faculty of Medicine, Muğla Sıtkı Koçman University, Muğla, Turkiye

Journal of Radiology in Medicine

Contents

Volume: 1 Issue: 4 Year: 2024

ORIGINAL ARTICLES

REVIEW

Journal of Radiology Medicine in

Original Article

Doi: 10.51271/JRM-0016

Contribution of automated hippocampal volume measurements to radiological diagnosis in cases of mesial temporal sclerosis

Kerime Hatun Acar[1], Ömer Faruk Sarıahmetoğlu[1], Serdar Arslan[1], Bora Korkmazer[1], Nil Çomunoğlu[2], Cihan İşler[3], Çiğdem Özkara[4], Osman Kızılkılıç[1]

[1]Department of Radiology, Cerrahpaşa Faculty of Medicine, İstanbul University-Cerrahpaşa, İstanbul, Turkiye
[2]Department of Pathology, Cerrahpaşa Faculty of Medicine, İstanbul University-Cerrahpaşa,İstanbul, Turkiye
[3]Department of Neurosurgery, Cerrahpaşa Faculty of Medicine, İstanbul University-Cerrahpaşa,İstanbul, Turkiye
[4]Department of Neurology, Cerrahpaşa Faculty of Medicine, İstanbul University-Cerrahpaşa,İstanbul, Turkiye

Received: 04.09.2024 ◆ **Accepted**: 08.10.2024 ◆ **Published**: 30.10.2024

Cite this article: Acar KH, Sarıahmetoğlu ÖF, Arslan S, et al. Contribution of automated hippocampal volume measurements to radiological diagnosis in cases of mesial temporal sclerosis. *J Radiol Med.* 2024;1(4):58-64.

Corresponding Author: Kerime Hatun Acar, kerimehozgen@gmail.com

ABSTRACT

Aims: Epilepsy, particularly drug-resistant epilepsy in adults, is often caused by mesial temporal sclerosis (MTS), which can develop after brain injury from febrile illnesses or trauma. Magnetic resonance imaging (MRI) is crucial for diagnosing MTS, although challenges such as patient movement and mild or bilateral hippocampal atrophy can complicate the diagnosis. T1-weighted hippocampal volume measurements are effective in detecting MTS, with recent software advancements enabling automatic hippocampal segmentation. This study compared the hippocampal volumes and indices between adults with MTS and a control group of similar age and sex in the Turkish population. This study aimed to highlight structural differences in the hippocampus associated with MTS.

Methods: This study involved a retrospective review of cranial MRIs scans from patients with MTS, confirmed through histopathological examination after epilepsy surgery. To ensure unbiased comparisons, a control group was selected using propensity score matching by age and gender. Two experienced neuroradiologists independently assessed the MRIs findings for MTS without knowledge of hippocampal volumetric data. Hippocampal volumes were measured using FreeSurfer software and standardized using the hippocampal volume index (HVI) and hippocampal asymmetry index (HAI).

Results: In our study of 38 patients, MTS was found in 55.2% of patients on the right side and in 44.8% of patients on the left side, with no bilateral cases. Visual MRI analysis identified MTS in 84.2% of patients, with an area under of curve (AUC) of 0.921. Automatic volumetry detected MTS in 23 patients with an AUC of 0.791. Combining both methods, MTS was diagnosed in 33 patients, with an AUC of 0.922.

Conclusion: Automated volumetric analyses have been shown to enhance the detection of hippocampal volume loss in patients with MTS.

Keywords: Mesial temporal sclerosis, hypocampus volume, automated segmentation

INTRODUCTION

Epilepsy is a significant health issue that affects both adults and children. In adults, the most common cause of drug-resistant epilepsy is mesial temporal sclerosis (MTS).[1] Many patients with MTS have a history of brain injury due to various factors, such as febrile illnesses or trauma. After an asymptomatic period, patients often develop refractory epilepsy.[2] The primary pathological changes that lead to seizure activity are epileptogenic foci in the mesial temporal region, which result from processes such as neuronal loss, hippocampal sclerosis, and axonal reorganization.[3,4] These changes can occur in isolation or in conjunction with other cortical malformation.

Patients diagnosed with MTS are usually treated with medications. However, approximately one-third of these patients do not respond to antiepileptic drugs. In such cases, surgery is a crucial option.[5] After determining the affected side of the brain, the most common surgical procedure involves removing the anterior part of the temporal lobe and mesial structures.[6] Magnetic resonance imaging (MRI) is widely

used to diagnose MTS. Typical MRI findings of MTS include hippocampal volume loss, increased signal intensity in the hippocampus on T2-weighted and FLAIR sequences, volume loss in the ipsilateral temporal lobe, reduced distinction between white and gray matter in the temporal lobe, and enlargement of the ipsilateral temporal horn.[7]

Different studies have reported varying MTS detection rates. Even expert radiologists sometimes find it challenging to identify MTS through radiological assessments, especially in cases of hippocampal degeneration.[8] Factors such as patient movement during imaging, signal intensity changes, or mild or bilateral hippocampal atrophy can complicate the diagnosis and lateralization of MTS, sometimes necessitating invasive monitoring.[9]

T1-weighted hippocampal volume measurements have long been proven effective in detecting MTS.[10] No significant differences exist between the hippocampal volume data obtained from 1.5T and 3T MRIs.[11] Previously volumetric data for hippocampal volume were obtained by manually segmenting consecutive slices, which is time-consuming and requires specialized expertise.[12] However, recent advances have enabled automatic hippocampal segmentation and volume measurement using various software packages, producing results comparable to those of manual methods in adult patients.[13] These software tools have simplified hippocampal volume measurement and are now used for diagnosing MTS, showing promising results, with sensitivity ranging from to 87-95%, specificity from to 57-94%, and accuracy from 82-89% to in clinical practice.[14] Furthermore, the hippocampal volume index (HVI) and hippocampal asymmetry index (HAI), used alone or together, have improved MRI's sensitivity, specificity, and predictive value of MRI in MTS diagnosis compared with other analytical techniques.[14]

Our study aimed to contribute to the literature by comparing hippocampal volumes, HAI, and HVI indices between individuals with histopathologically confirmed MTS and a control group of similar age and sex within the adult Turkish population.

METHODS

Study Design

Our study was conducted by retrospectively reviewing the cranial MRIs of patients diagnosed with mesial temporal sclerosis (MTS) through histopathological examination following surgery for refractory epilepsy. These patients presented to the epilepsy outpatient clinic of the neurology department at our institution between January 2019 and June 2024. The study was approved by the İstanbul University-Cerrahpaşa Clinical Researches Ethics Committee (Date:18.09.2024, Decision No: 1090171). All procedures were carried out in accordance with the ethical rules and the principles of the Declaration of Helsinki.

Patient Enrollment

We included patients who had undergone surgery for refractory epilepsy, had histopathologically confirmed diagnoses, and whose medical records and imaging data were available at our institution. Patients were excluded if the retrospective review of the pathological results revealed any conditions that could cause epilepsy, such as intracranial malignancy, encephalomalacia, previous intracranial surgery, cortical malformations, or cortical dysplasia. A total of 52 patients met the inclusion criteria. However, upon reviewing their radiological images within our institution's PACS system (Extreme PACS, Ankara), 14 patients were excluded because they did not have MRI scans that adhered to the epilepsy protocol. Consequently, 38 patients were included in the final study.

To avoid bias when compared to the MTS group, we applied propensity score matching by age and sex to select a control group. After matching, 42 control subjects with regular radiological reports and T1 volumetric sections suitable for automatic segmentation using our PACS system were included.

Magetic Resonance Imaging Protocols

All patients underwent MRI scans using a 3T Intera Achieva scanner (Philips Healthcare, Best, Netherlands) following the epilepsy imaging protocol, which included: Coronal images perpendicular to the long axis of the hippocampus, identified on the sagittal plane: 1) T2-weighted imaging (3 mm slice thickness, no gap, voxel size=0.89 x 1 x 3 mm, TR=3300 ms, TE=30/60/90/120/150 ms, matrix=200x180, FOV=180x180, TSE factor=5; EPI factor=5, flip angle=90°); 2) T1-weighted inversion recovery (3 mm slice thickness, no gap, voxel size=0.75x0.75x3 mm, TR=3550 ms, TE=15 ms, TI=400 ms, matrix=240x229, FO=180x180, TSE factor=7); 3) FLAIR (spectral-attenuated inversion recovery, fat suppression power=1, 4 mm slice thickness, section gap=1 mm, voxel size=0.89x1.1x2.4 mm, TR=12,000 ms, TE=140 ms, TI=2850 ms, matrix=180x440, FOV=200x200). Axial images parallel to the long axis of the hippocampus: FLAIR (fat-suppressed spectral-attenuated inversion recovery, 4 mm slice thickness, section gap=1 mm, voxel size=0.89x1.1x2.4 mm, TR=12,000 ms, TE=140 ms, TI=2850 ms, matrix=224x160, FOV=200x200). T1-weighted volumetric images: isotropic voxels of 1 mm, acquired in the sagittal plane (1 mm slice thickness, no gap, flip angle=8°, TR=7.0 ms, TE=3.2 ms, matrix=240×240, FOV=240×240). T2-weighted volumetric images: isotropic voxels of 1.5 mm, acquired in the sagittal plane (no gap, TR=1800 ms, TE=340 ms, matrix=140x140, FOV=230x230, TSE factor=20; flip angle=90°; geometry corrected).

Imaging Analysis

Two board-certified neuroradiologists with 12 and 20 years of experience (S.A. and O.K.) independently reviewed the MRIs, blinded to the hippocampal volumetric data. They assessed the presence of MTS findings, such as hippocampal atrophy, gliosis, and signal changes in the mesial temporal region. If other abnormalities were observed in the mesial temporal structures, they were asked to note them. In cases of disagreement, a final decision was reached through a consensus after a joint review.

Hippocampal Volume Measurement

Hippocampal volume measurements were performed using T1-weighted images on a personal computer equipped with an AMD Ryzen 5 Pro 3.7 GHz processor, 16 GB RAM, and Windows 10, using FreeSurfer software (version 7.4.1; http://surfer.nmr.mgh.harvard.edu), which performs automatic reconstruction and segmentation. The procedures included removing non-brain tissue using a hybrid watershed algorithm,

automatic transformation to the Talairach reference space, and segmentation of subcortical white matter and deep gray matter structures. The entire hippocampal formation was segmented using a standard procedure and a probabilistic brain atlas. The estimated intracranial volume (ICV) was calculated for each subject[15] (**Figure 1**).

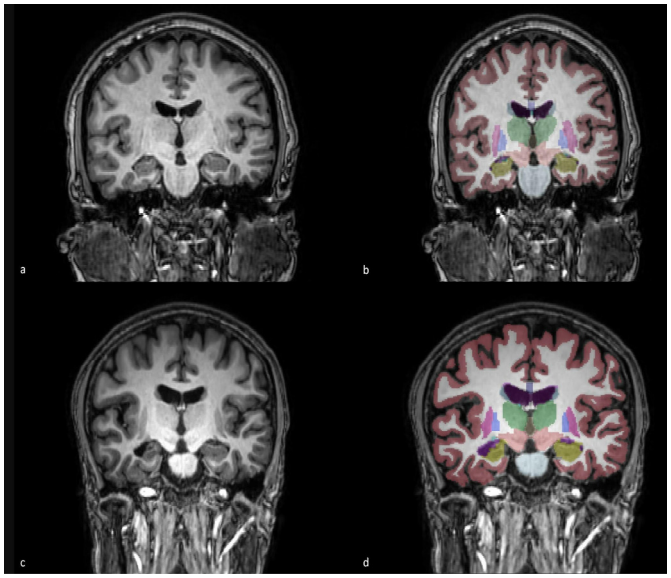

Figure 1. a,b. A 38-year-old healthy individual. **a.** Cranial MRI T1-weighted images (T1WI) in coronal sections displaying both hippocampi. **b.** FreeSurfer segmented image illustrating brain cortical and subcortical structures, with both hippocampi highlighted in yellow and the lateral ventricular temporal horn in purple. **c,d**. A 28-year-old male patient diagnosed with right mesial temporal sclerosis (MTS). MR imaging volumetry revealed a significant reduction in the volume of the right hippocampus. **c.** T1WI showing both hippocampi, which appear normal upon visual inspection. **d.** FreeSurfer volumetry images with the hippocampi marked in yellow. The right hippocampus is notably smaller than the left, and the right lateral ventricular temporal horn (purple) is visibly wider than the left.

Data Analysis

Volumetric values were standardized using the hippocampal volume index (HVI), which is the ratio of the hippocampal volume to the total intracranial volume (TIV) (HVI=hippocampal volume/TIV×100). Separate values were obtained for the right hippocampus (HVIR) and the left hippocampus (HVIL). Interhemispheric comparisons were performed using the hippocampal asymmetry index (HAI), defined as the difference between the left and right hippocampal volumetric indices, and the sum of these indices (HAI=[HVIL-HVIR]/[HVIR+HVIL]). Atrophy was considered if there was a difference of more than 2 SD between the measured volumetric values and indices and the mean values of the controls. In addition, we combined the performance of neuroradiologists with automatic volumetric measurements. A patient was considered to have MTS if either or both the methods yielded positive results.

Statistical Analysis

Categorical data were presented as numbers and percentages (N, %) and compared using Pearson's Chi-square or Fisher's exact test, where appropriate. Numerical values are presented as mean and standard deviation. Two independent-sample t-tests were used to determine whether the parametric values showed a statistically significant difference. The Shapiro-Wilk test was used to ensure that the data were normally distributed. The specificity and sensitivity of the values were calculated and ROC curve analysis was performed for each lateralization assessment. Statistical significance was considered two-tailed ($p<0.05$). Statistical analysis was conducted using IBM Statistical Package for the Social Sciences (SPSS) version 22.0 for Windows.

RESULTS

In our study, 29% (5/17) of cases were excluded due to lack of imaging studies,; another 29% (5/17) were excluded due to accompanying pathologies such as focal cortical dysplasia, 24% (4/17) were excluded due to extensive tissue loss caused by preoperative changes such as encephalomalacia and infarction, and 18% (3/17) were excluded due to the detection of intracranial malignancy. A total of 38 patients met the inclusion criteria (**Table 1**).

MTS was detected on the right side in 21 patients (55.2%) and on the left side in 17 (44.8%). There were no cases of bilateral MTS. The patient group consisted of 21 females (55.3%) and 17 males (44.7%), with an average age of 34.29±10.02 years. The control group consisted of 42 individuals, 21 females (50%) and 21 males (50%), with an average age of 34.62±11.01 years (**Table 2**).

No significant differences were found between patients and controls in terms of sex and age distribution (sex, $p=0.661$; age, $p=0.502$). No significant relationship was found between the sex of the patient and the side of the lesion ($p=0.796$). Regarding sex, no significant differences were found in the adjusted HVIR and HVIL values in control subjects (HVIR, $p=0.091$; HVIL, $p=0.107$) (**Table 2**).

Neuroradiologists' Evaluation

Excellent concordance was observed among the neuroradiologists. In evaluating the MTS, both radiologists provided positive interpretations for 30 patients. In contrast, in one patient, the O.K. was negative, S.A. was positive, O.K. was positive, and S.A. was negative. In these two patients, a decision favoring the disease was made based on a joint assessment. The results showed that 32 individuals (84.2%) were consistent with MTS in the visual analyses on MRI. Despite the presence of MTS in the visual analysis, MTS was not detected in 6 patients (15.8%). The area under the curve for joint neuroradiologist assessment was 0.921 (standard error 0.036, $p<0.001$; 95% CI).

Automated Volumetry

In the control group, the average right hippocampal volume was 4236.36±452.32 mm^3, while the average left hippocampal volume was 4102.83±422.11 mm^3. The mean HVIR was 0.301±0.031, and 0.292±0.031 in the control and HVIL groups, respectively. For controls, the mean HAI index in absolute terms was 0.027±0.018. Automatic volume measurement revealed physiological asymmetry between the right and left hippocampal volumes in the control group, with the right hippocampal volume being 3.3% larger than the left ($p<0.001$). In the patient group, the average right hippocampal volume was 3755.41±802.51 mm^3, while the average left hippocampal volume was 3899.12±610.49 mm^3. The mean HVIR in the patient group was 0.457±0.28, and the mean HVIL was 0.426±0.29. The mean HAI index in the patients was 0.840±0.370, which was significantly higher than that in the control group ($p<0.001$). Right hippocampal volumes were significantly reduced in patients with right MTS compared to those without right MTS ($p<0.001$). Similarly, left hippocampal volumes were significantly reduced in patients with left MTS compared to those without left MTS ($p=0.006$).

Table 1. MTS group

Patient	Age (years)	Sex	MTS	Hippocampus (R)	Hippocampus (L)	TVI	HVIR	HVIL	HAI
1	41	M	R	1822.6	3991.7	1370900.3	0.21	0.29	0.14
2	34	F	R	2098.8	4102	1208412.1	0.36	0.33	-0.03
3	19	F	R	1298.6	3.642	956790.83	0.37	0.38	0.00
4	56	F	R	1752.4	3604.9	1389013.7	0.20	0.25	0.11
5	28	F	L	1126.9	2861.4	1050819.5	0.37	0.27	-0.16
6	28	M	R	2059.1	4544.6	1701792.3	0.20	0.26	0.13
7	32	F	R	2151.5	4305.5	1034469.3	0.45	0.41	-0.04
8	23	F	R	1796.7	4015.9	1548279.2	0.20	0.25	0.10
9	49	F	L	2116.8	4058.1	1640752.9	0.31	0.24	-0.12
10	23	F	R	2127.4	4597.3	1445610.6	0.34	0.31	-0.04
11	32	F	R	2072.2	3834.6	1169270.2	0.34	0.32	-0.02
12	24	M	L	2116.1	4470.2	1643794	0.27	0.27	0.00
13	35	F	L	1895.1	4337.9	1314324.7	0.34	0.33	-0.02
14	34	M	L	2094.6	4868.2	1641647.8	0.30	0.29	-0.01
15	28	M	R	1878.8	4652.1	1183510.2	0.30	0.39	0.12
16	21	M	R	1900.5	4145.9	1599950.2	0.19	0.25	0.13
17	41	F	L	1844.5	4116.3	1415082.4	0.30	0.29	-0.02
18	29	F	L	1835.7	2559.9	1252275.6	0.31	0.20	-0.21
19	35	F	R	1407.5	3371.6	791471.61	0.35	0.42	0.09
20	46	M	R	1971.4	4180	1474052.8	0.25	0.28	-0.04
21	48	F	L	1586.3	4354.8	1395354.1	0.32	0.31	-0.01
22	48	M	L	1832.7	4141.1	1820314.1	0.25	0.22	-0.05
23	57	F	R	1752.9	3707.8	994663.37	0.33	0.37	0.05
24	37	M	L	1590.1	2630.2	1380438.2	0.19	0.19	-0.02
25	32	F	L	1359.5	3133.7	1079315.7	0.30	0.29	-0.02
26	40	M	L	1374.6	3428.9	1092095.6	0.30	0.31	0.01
27	26	M	R	1676.2	4128.3	1491270.7	0.18	0.27	0.18
28	45	F	L	2253.1	3122.3	1254046.5	0.37	0.24	-0.20
29	47	F	L	1215.7	3728.3	1182686.6	0.30	0.31	0.01
30	25	M	R	649.3	4381.6	1846007.9	0.15	0.23	0.21
31	37	M	R	2515	4971.3	1540049.3	0.28	0.32	0.06
32	33	F	R	1255.9	4048.2	1412347.7	0.20	0.28	0.16
33	29	M	L	2009.3	3064.6	1286119.9	0.29	0.23	-0.10
34	33	F	R	1886.7	4293.5	1444513.1	0.26	0.29	0.06
35	18	M	R	481.4	4245.4	1455397.5	0.12	0.29	0.40
36	25	M	L	1992.7	3619.6	1687706.2	0.26	0.21	-0.10
37	40	F	R	1507.1	4108.7	1353613	0.19	0.30	0.21
38	25	M	L	1448.9	2798.5	1497254.9	0.26	0.18	-0.16

Table 2: Control group

Patient	Age (years)	Sex	MTS	Hippocampus (R)	Hippocampus (L)	TVI	HVIR	HVIL	HAI
1	35	F	0	3304.2	3177	1107147.9	0.29	0.28	-0.01
2	23	M	0	4341.7	4159	1350956.2	0.31	0.30	-0.02
3	21	F	0	3964	3890.3	1429430.9	0.27	0.27	0.00
4	34	M	0	5020.2	4348.9	1524919.7	0.32	0.28	-0.07
5	26	F	0	4139.8	4524.3	1474817.2	0.28	0.30	0.04
6	28	F	0	4131.6	4091.6	1314065.8	0.31	0.31	0.00
7	32	F	0	4898.6	4638.6	1447987.2	0.33	0.32	-0.02
8	33	F	0	3804.9	3664.8	1061439.7	0.35	0.34	-0.01
9	19	M	0	4391.7	3911.3	1635988.5	0.26	0.23	-0.05
10	19	M	0	4796.2	5044.1	1695725.3	0.28	0.29	0.02
11	35	M	0	4802.8	4473	1648093.6	0.29	0.27	-0.03
12	38	F	0	3331.5	3389.4	1333834.4	0.24	0.25	0.00
13	43	M	0	4815.1	4414.7	1372317.9	0.35	0.32	-0.04
14	50	F	0	3727.7	3644.3	1460117	0.25	0.24	-0.01
15	56	F	0	4186.9	3942.3	1361931.9	0.30	0.28	-0.03
16	46	M	0	4310.1	4027.3	1536389.8	0.28	0.26	-0.03
17	45	M	0	4108.6	4566.1	1563843.8	0.26	0.29	0.05
18	39	F	0	3421.8	3301.7	1045933.7	0.32	0.31	-0.01
19	32	F	0	4413	4263.5	1209318	0.36	0.35	-0.01
20	31	F	0	4733.9	4275.8	1517097.7	0.31	0.28	-0.05
21	28	M	0	4397.8	4365	1482867.8	0.29	0.29	0.00
22	23	M	0	4823.3	4569.8	1636038.5	0.29	0.27	-0.02
23	23	M	0	4074	4175	1477876.1	0.27	0.28	0.01
24	26	M	0	4735	4119.5	1689085.7	0.28	0.24	-0.06
25	29	M	0	4114.6	4338.8	1323723.1	0.31	0.32	0.02
26	30	M	0	4462.3	4249.1	1574831.4	0.28	0.26	-0.02
27	35	F	0	4321	3849.5	1351729.5	0.31	0.28	-0.05
28	35	M	0	4462.3	4249.1	1574831.4	0.28	0.26	-0.02
29	42	M	0	4420.8	4138	1572328.1	0.28	0.26	-0.03
30	48	M	0	4283.3	4259	1461063	0.29	0.29	0.00
31	58	F	0	3778.5	3935.1	1393277.6	0.27	0.28	0.02
32	29	M	0	4688.6	5074.7	1495213.7	0.31	0.33	0.03
33	43	F	0	3786.3	3596.8	1316671.7	0.28	0.27	-0.02
34	45	F	0	4045.3	3820.2	1338679.1	0.30	0.28	-0.02
35	37	F	0	4851.3	4371.7	1653291.2	0.29	0.26	-0.05
36	50	F	0	3747.6	3606.3	1316642.8	0.28	0.27	-0.01
37	22	F	0	4087.3	3992.3	1094632.8	0.37	0.36	-0.01
38	57	F	0	3551.7	3529.7	1135889.3	0.31	0.31	0.00
39	28	M	0	3533.7	3666.4	1426506.9	0.24	0.25	0.01
40	19	M	0	4255	3875.8	1295258.8	0.32	0.29	-0.04
41	18	F	0	4440.6	4426.7	1188054.3	0.37	0.37	0.00
42	44	M	0	4422.6	4362.4	1599046.9	0.27	0.27	0.00

F: Famale, M: Male, MTS: Mesial Temporal Sclerosis, HVIR: Right hippocampus, HVIL: Left hippocampus, HAI: Hippocampal asymmetry index

Table 3. Demographic characteristics

	Patients (n:38)	Controls (n:42)	p value
Age (years)	34.29±10.02	34.62±11.01	0.502
Gender (male)	44.7% (n: 17)	50% (n:21)	0,661
Side of MTS	Left: 44.8 (n:17) Right: 55.2% (n:21)		

MTS: Mesial temporal sclerosis

The threshold for diagnosing MTS was set at a difference of 0.059 or higher for the HAI. Additionally, values of 0.239 or lower for HVIR and 0.231 or lower for HVIL were considered significant for the MTS. Based on the HVI values, 16 patients were diagnosed with MTS, with no misdiagnoses in the control group. In the HVI analysis, an area under the curve (AUC) of 0.711 was obtained for the diagnosis and lateralization of patients with MTS, with a sensitivity of 42.0% and specificity of 100.0% (standard error 0.060, p=0.001; 95% CI). HAI correctly identified 21 patients with MTS using the automatic method but incorrectly diagnosed one control as MTS. The predictive values were better with the HAI. For the HAI values, an area under the curve of 0.764 was obtained, with a sensitivity of 55.00% and specificity of 97% (standard error 0.056, p<0.001; 95% CI). Among the seven patients identified with MTS based on HAI values, the HVI values were within normal limits, and two patients with average HAI values had HVI values consistent with MTS. In 14 patients, both HAI and HVI values consistently indicated MTS, whereas 15 patients were within normal limits for both indices. In the automatic volumetric analysis, MTS was detected in 23 patients based on the overall performance of the HVI or HAI indices. The area under the curve for automatic volumetry was 0.791 (standard error 0.054; p<0.001; 95% CI).

Overall Performance

Visual inspection and automatic volumetry detected mesial temporal sclerosis (MTS) in 22 patients. However, both methods missed MTS in 5 patients, resulting in false-negative outcomes. Overall, the two methods were in agreement in 27 of the 38 cases. Among the ten patients with visually identified MTS, 95% had average volumetric indices, whereas 13% of those with visually averaged MRI results showed hippocampal atrophy through volumetric analysis. MTS was diagnosed in 33 patients when both methods were combined. The area under the curve (AUC) for the combined effectiveness of visual assessment and automatic volumetry was 0.934 (standard error 0.033, p<0.001; 95% CI) (**Figure 2**).

DISCUSSION

MTS is the primary cause of refractory epilepsy. According to the literature, 55.5% of these patients show findings consistent with MTS, based on tests and examinations.[16,17] MRI is beneficial and commonly used for identifying epilepsy-related pathologies, such as MTS.[18] Furthermore, detecting MRI findings of hippocampal sclerosis, the primary pathology in MTS, is crucial for determining lateralization in drug-resistant MTS patients and for guiding surgical treatment.[19] Typical imaging findings of MTS include signal changes in T2-weighted sequences and decreased hippocampal size.[20] Additionally, hippocampal volume data are recognized as reliable surrogate markers for hippocampal sclerosis, the primary pathological basis of MTS.[21]

Many neuroradiologists are adept at visually identifying moderate-to-severe hippocampal atrophy when conducting epilepsy MRI protocols. However, detecting MRI abnormalities in patients with MTS relies heavily on both the quality of the MRI protocol and the evaluator's experience in interpreting MRIs in patients with epilepsy. In a particular study, "non-expert" radiologists deemed 61% of specific standard MRIs as normal, whereas "expert" radiologists found that 28% of the same MRIs were technically inadequate and 22% were normal.[22] It has been demonstrated that even expert neuroradiologists can produce false-negative results with qualitative analysis when there are varying conditions related to the imaging technique and patients.[9] Additionally, qualitative MRI readings may miss minor differences in hippocampal volumes, and quantitative volume measurements have been reported to be beneficial in such cases.[23] The strong correlation between the volumes detected by quantitative analysis and histopathology supports this hypothesis.

Recent research has indicated that measuring hippocampal volume can aid qualitative analysis in cases of mild hippocampal volume loss,[24] bilateral hippocampal volume loss with minimal

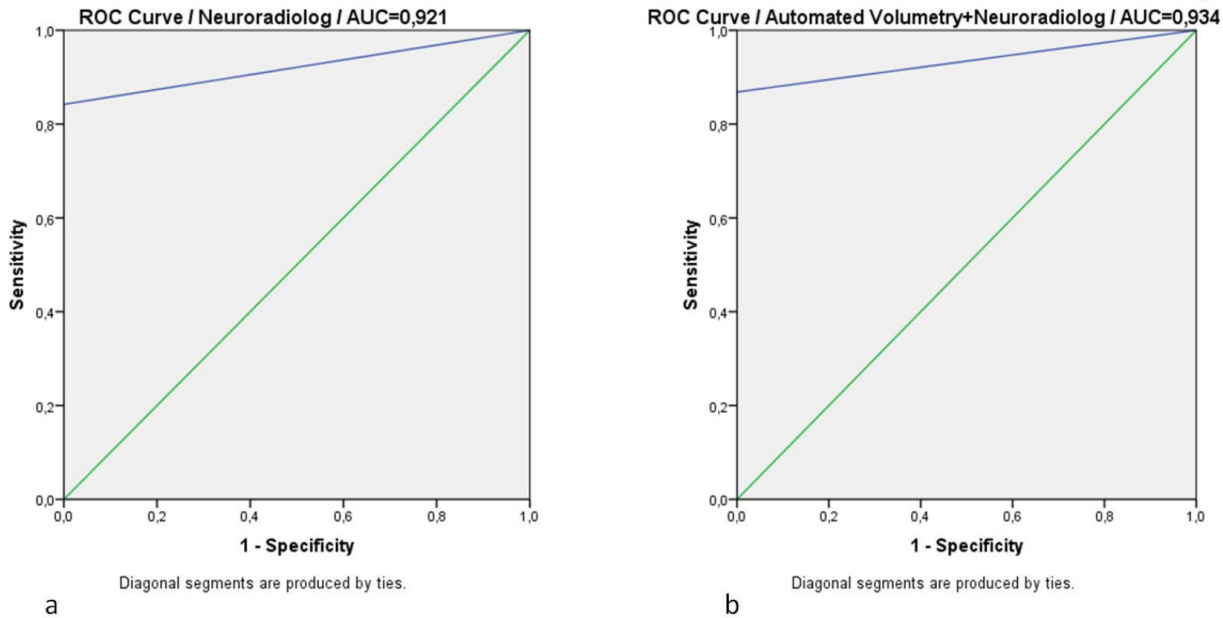

Figure 2. The Receiver Operating Characteristic (ROC) curve analysis for diagnosing mesial temporal sclerosis indicates that combining automated volumetry with visual assessment enhances the area under the curve (AUC). This suggests improved diagnostic accuracy when both methods are used together.

or no asymmetry,[25] and in centers without expertise in epilepsy imaging.[26]

Studies have shown that manually measured hippocampal volumes are more accurate than those measured using automatic methods. However, automatic segmentation is approximately 77% faster than manual segmentation and is less susceptible to different operator biases.[26-28] Additionally, the small size of the hippocampus can lead to significant errors in volume calculation during manual measurements.[21] The literature also suggests that results from FreeSurfer software, which automatically performs cerebral cortex parcellation and subcortical structure segmentation based on probabilistic information from manual segmentation datasets, can be as reliable as those obtained through manual techniques.[14,29] Therefore, we used the FreeSurfer software to obtain hippocampal volume data.

Through volume analysis conducted on healthy controls, we found that the hippocampal volumes (right=4236 mm^3, left=4102 mm^3) were consistent with the values obtained in a previous study[19] using a similar software and methodology (right=4179 mm^3, left=3999 mm^3). This consistency indicates the reproducibility of the automatic segmentation. The left dominance observed in our study might be a physiological characteristic of our population; however, more extensive cohort studies are needed to confirm this hypothesis. Furthermore, as reported in the literature, no statistically significant differences were observed in hippocampal values between sexes or HVI values between the right and left hemispheres in the control group.[30]

In previous studies, evaluating hippocampal atrophy using HVI values yielded a sensitivity between 44% and 94% and a specificity between 86% and 96%. When HAI values were utilized, sensitivity ranged from 88% to 96%, and specificity ranged from 87% to 100%. In our study, using threshold values determined by ROC analysis, we achieved sensitivity and specificity for detecting hippocampal volume loss, consistent with the literature, based on both HVI and HAI values. Pathology reports indicated a significant correlation between the side where MTS was detected and the side where volume loss was observed. However, contrary to our expectations, we observed a slight increase in hippocampal volume on the affected side in six patients. This suggests that during the very early stages of the disease, before atrophy develops, the hippocampal volume may temporarily increase due to inflammatory changes.[31] This might be one of the reasons why the sensitivity and specificity of the threshold values calculated in our study are lower than those reported in the literature.

In alignment with a similar study conducted previously in a different population, our research found that the predictive value of HAI was superior. HAI demonstrated a higher true-positive rate and a lower false-negative rate than HVI. Furthermore, the absolute threshold value for HAI identified in this study (0.06) closely matched the absolute threshold value that we determined (0.057). This suggests that the HAI value does not vary significantly across different populations, and is reliable in terms of reproducibility. Physiological asymmetry between hippocampal volumes has been consistently reported in various studies.[9,32]

The neuroradiologist's assessments demonstrated sensitivity and specificity rates comparable to those in other studies with similar goals.[9,20] When automatic volumetric values were evaluated in coordination with neuroradiologists, there was a notable increase in both the sensitivity and specificity. Furthermore, the excellent specificity rate observed in our study supports the clinical application of the workflow proposed in a previous study.[20] The main reason for achieving similar results in both studies might be the difficulty in visually detecting minor volumetric differences.[23]

Limitations

The main limitations of this study are the small cohort size and retrospective nature of the analysis. Second, hippocampal atrophy is only one component of MTS, and signal changes in T2-weighted FLAIR images are among the other findings of hippocampal sclerosis. However, the detection of T2-weighted signal changes in pathologies, such as focal cortical dysplasia and temporal lobe lesions causing epilepsy, apart from MTS, indicates that hippocampal volume loss is a more specific marker for MTS. Additionally, the neuroradiologist interpreting the study might have been biased because of being aware of the patient's clinical diagnosis of epilepsy. However, the quantitative MRI data were blinded to the control subjects and patients. Finally, our dataset was relatively small to determine the optimal threshold values, and there was notable asymmetry in the hippocampal volume ratios within the population we studied. Additionally, differences in hippocampal volume size were observed based on the timing of potential MTS pathology. Therefore, the absolute optimal threshold value may vary with the lateralization of pathology.

Automated volumetric analyses have been shown to enhance the detection of hippocampal volume loss in MTS patients. By incorporating these efficient volumetric methods, which can be identified via MRI, into clinical workflows, radiological assessments can be streamlined. Moreover, with further validation, these methods can evolve into parameters that clinicians can interpret in routine practice. Additionally, combining hippocampal volume measurements with data from other imaging techniques, such as T2 and FLAIR in future studies, which include larger patient and control groups, offers exciting potential for improving the effectiveness of clinical applications.

CONCLUSION

In conclusion, the qualitative analysis of signal changes in T2-weighted and FLAIR imaging, combined with unbiased quantitative volumetric data, facilitates a more comprehensive investigation of the critical findings in hippocampal sclerosis pathology.

ETHICAL DECLARATIONS

Ethics Committee Approval

The study was carried out with the permission of the Faculty of İstanbul University-Cerrahpaşa Clinical Researches Ethics Committe (Date: 18.09.2024, Decision No: 1090171).

Informed Consent

Because the study was designed retrospectively, no written informed consent form was obtained from patients.

Referee Evaluation Process

Externally peer-reviewed.

Conflict of Interest Statement

The authors have no conflicts of interest to declare.

Financial Disclosure

The authors declared that this study has received no financial support.

Author Contributions

All of the authors declare that they have all participated in the design, execution, and analysis of the paper, and that they have approved the final version.

REFERENCES

1. Blumcke I. Neuropathology of focal epilepsies: a critical review. *Epilepsy Behav*. 2009;15(1):34-39.
2. French JA, Williamson PD, Thadani VM, et al. Characteristics of medial temporal lobe epilepsy: I. Results of history and physical examination. *Ann Neurol.* 1993;34(6):774-780.
3. Thom, M. Hippocampal sclerosis in epilepsy. *Neuropathol Appl Neurobiol.* 2014;40(5):520-543. doi:10.1111/nan.12150
4. Barkovich AJ, Kuzniecky RI: Neuroimaging of focal malformations of cortical development. *J Clin Neurophysiol*. 1996;13(6):481-494.
5. Jones AL, Cascino GD. Evidence on use of neuroimaging for surgical treatment of temporal lobe epilepsy: a systematic review. *JAMA Neurol.* 2016;73(4):464-470.
6. Ramey WL, Martirosyan NL, Lieu CM, et al. Current management and surgical outcomes of medically intractable epilepsy. *Clin Neurol Neurosurg.* 2013;115(12):2411-2418.
7. Jack CR Jr, Sharbrough FW, Twomey CK, et al. Temporal lobe seizures: lateralization with MR volume measurements of the hippo campal formation. *Radiology*. 1990;175(2):423-429.
8. Farid N, Girard HM, Kemmotsu N, et al. Temporal lobe epilepsy: quantitative MR volumetry in detection of hippocampal atrophy. *Radiology.* 2012;264(2):542-550.
9. Farid N, Girard HM, Kemmotsu N, et al. Temporal lobe epilepsy: quantitative MR volumetry in detection of hippocampal atrophy. *Radiology*. 2012; 264(2):542–550
10. Van Paesschen W, Sisodiya S, Connelly A, et al. Quantitative hippocampal MRI and intractable temporal lobe epilepsy. *Neurology*. 1995;45(12):2233-2240.
11. Briellmann, RS, Syngeniotis, A, Jackson, GD. Comparison of hippocampal volumetry at 1.5 T and at 3 T. *Epilepsia*. 2001;42(8):1021-1022
12. Cherbuin N, Anstey KJ, Reglade-Meslin C, et al. In vivo hippocampal measurement and memory: a comparison of manual tracing and automated segmentation in a large community-based sample. *PloS One*. 2009;4(4):e5265.
13. Tae WS, Kim SS, Lee KU, et al. Validation of hippocampal volumes measured using a manual method and two automated methods (FreeSurfer and IBASPM) in chronic major depressive disorder. *Neuroradiology.* 2008; 50(7):569-581.
14. Granados Sánchez AM, Orejuela Zapata JF. Diagnosis of mesial temporal sclerosis: sensitivity, specificity and predictive values of the quantitative analysis of magnetic resonance imaging. *Neuroradiol J*. 2018;31(1):50-59. doi:10.1177/1971400917731301
15. Fischl B, Salat DH, Busa E, et al. Whole Brain segmentation: automated labeling of neuroanatomical structures in the human brain. *Neuron*. 2002; 33(3):341-355. doi: 10.1016/S0896-6273(02)00569-X
16. Granados A, Orejuela J, Rodriguez-Takeuchi S. Neuroimaging evaluation in refractory epilepsy. *Neuroradiol J.* 2015;28(5):529-535.
17. Jette N, Wiebe S. Update on the surgical treatment of epilepsy. *Curr Opin Neurol*. 2013;26(2):201-207.
18. McLachlan RS, Nicholson RL, Black S, et al. Nuclear magnetic resonance imaging, a new approach to the investigation of refractory temporal lobe epilepsy. *Epilepsia* 1985;26(6):555-562.
19. Coan AC, Kubota B, Bergo FPG, et al. 3T MRI quantification of hippocampal volume and signal in mesial temporal lobe epilepsy improves detection of hippocampal sclerosis. *Am J Neuroradiol*. 2014;35(1):77-83.
20. Silva G, Martins C, Moreira da Silva N, et al. Automated volumetry of hippocampus is useful to confirm unilateral mesial temporal sclerosis in patients with radiologically positive findings. *Neuroradiol J*. 2017;30(4):318-323.
21. Azab M, Carone M, Ying SH, et al. Mesial temporal sclerosis: accuracy of NeuroQuant versus neuroradiologist. *AJNR Am J Neuroradiol.* 2015;36(8): 1400-1406.
22. Von Oertzen J, Urbach H, Jungbluth S, et al. Standard magnetic resonance imaging is inadequate for patients with refractory focal epilepsy. *J Neurol Neurosurg Psychiatry*. 2002;73(6):643-647.
23. Ono SE, de Carvalho Neto A, Joaquim MJM, Dos Santos GR, de Paola L, Silvado CES. Mesial temporal lobe epilepsy: revisiting the relation of hippocampal volumetry with memory deficits. *Epilepsy Behav*. 2019;100(Pt A):106516. doi: 10.1016/j.yebeh.2019.106516
24. Reutens DC, Stevens JM, Kingsley D, et al. Reliability of visual inspection for detection of volumetric hippocampal asymmetry. *Neuroradiology.* 1996; 38(3):221-225.
25. Akhondi-Asl A, Jafari-Khouzani K, Elise vich K, Soltanian-Zadeh H. Hippocampal volumetry for lateralization of temporal lobe epilepsy: automated versus manual methods. *Neuroimage*. 2011;54(Suppl 1):218-226.
26. Pardoe HR, Pell GS, Abbott DF, Jackson GD. Hippocampal volume assessmentintem poral lobe epilepsy: how good is automated segmentation? *Epilepsia*. 2009;50(12):2586-2592.
27. Silva NM, Rozanski VE, Cunha JPS. A 3D multi modal approach to precisely locate DBS electrodes in the basal ganglia brain region. 2015 7th International IEEE/EMBS Conference on Neural Engineering (NER). 2015;pp.292-295.
28. Hsu YY, Schuff N, Du AT, et al. Comparison of automated and manual MRI volumetry of hippocampus in normal aging and dementia. *J Magn Reson Imag: JMRI*. 2002;16(3):305-310.
29. Wenger E, Martensson J, Noack H, et al. Comparing manual and automatic segmentation of hippocampal volumes: reliability and validity issues in younger and older brains. *Human Brain Mapping*. 2014;35(8):4236-4248.
30. Akos-Szabo C, Xiong J, Lancaster JL, et al. Amygdalar and hippocampal volumetry in control participants: differences regarding handedness. *AJNR Am J Neuroradiol*. 2001;22(7):1342-1345.
31. Ashtari M, Barr WB, Schaul N, et al. Three-dimensional fast low-angle shot imaging and computerized volume measurement of the hippocampus in patients with chronic epilepsy of the temporal lobe. *AJNR Am J Neuroradiol*. 1991;12(5):941-947.
32. Mohandas AN, Bharath RD, Prathyusha PV, et al. Hippocampal volumetry: normative data in the Indian population. *Ann Ind Acad Neurol*. 2014;17(3):267-271.

Journal of Radiology Medicine in

Original Article

Doi: 10.51271/JRM-0017

Doppler findings before and after endovascular treatment in peripheral artery disease

Yunus Yılmazsoy, Samet Genez, Hamza Özer, Sümeyra Nur Atasoy

Department of Radiology, Faculty of Medicine, Bolu Abant İzzet Baysal University, Bolu, Turkiye

Received: 30.09.2024 ◆ **Accepted**: 17.10.2024 ◆ **Published**: 30.10.2024

Cite this article: Yılmazsoy Y, Genez S, Özer H, Atasoy SN. Doppler findings before and after endovascular treatment in peripheral artery disease. *J Radiol Med.* 2024;1(4):65-68.

Corresponding Author: Yunus Yılmazsoy, yunusyilmazsoy@gmail.com

ABSTRACT

Aims: Peripheral arterial disease is a significant health problem affecting approximately 50 million people in the United States and Europe, which can lead to disability, limb loss, and poor quality of life. This is the main cause of significant morbidity and mortality. In this study, we aimed to share our early Doppler findings in patients who underwent endovascular procedures in our clinic.

Methods: The radiological findings of 9 patients who applied to our clinic and treated with endovascular interventional methods in the last 6 months were evaluated retrospectively and the results were analyzed with descriptive statistical methods.

Results: Patients with peripheral arterial occlusion or sever stenosis treated with endovascular treatment showed significant increase in lower extremity arterial flow evaluated by color Doppler ultrasound regardless of endovascular technique.

Conclusion: Doppler ultrasonography is a useful technique showing increase of the flow dynamics before and after the successful endovascular treatment procedure of lower extremity peripheral arterial disease are a method that provides useful data to predict outcome of the patients.

Keywords: Peripheral arterial disease, Doppler ultrasound, endovascular treatment

INTRODUCTION

Peripheral artery disease is a significant health problem affecting approximately 50 million people in the United States and Europe, leading to disability, limb loss, and diminished quality of life.[1] It predominantly affects individuals over 50 years of age, with incidence increasing with age.

Risk factors for PAD include advanced age, male gender, obesity, sedentary lifestyle, hyperlipidemia, low HDL levels, hypertension, smoking, diabetes mellitus, coronary artery disease, renal failure, elevated fibrinogen levels, hypercoagulability, hyperhomocysteinemia, elevated CRP levels, and family history of cardiovascular disease, which are typical of atherosclerotic diseases.[2-4]

Atherosclerosis is a systemic disease closely associated with cardiovascular and cerebrovascular diseases.[5,6] The prevalence of cardiovascular disease in patients with peripheral artery disease is 2-3 times higher, contributing significantly to morbidity and mortality.[7]

Many patients with PAD are asymptomatic. Intermittent claudication is the most common symptom in symptomatic cases, and more severe cases may involve tissue loss.[8]

Treatment options for peripheral artery disease include endovascular procedures such as balloon angioplasty, stenting, plaque aspiration, thrombolysis, percutaneous thrombectomy, as well as surgical methods like autogenous-synthetic bypasses and endarterectomy.[9] With advancements in technique and technology, endovascular procedures are increasingly preferred over open vascular bypass surgery.

Literature discusses the advantages and disadvantages of endovascular techniques. Advantages include less invasiveness, low complication rates, shorter hospital stays, and lower costs, while disadvantages include less suitability for long segment lesions and disease recurrence.[10]

In this study, we aimed to share our Doppler findings before and after endovascular procedures of patients with lower limb ischemia.

METHODS

After the Bolu Abant İzzet Baysal University Faculty of Medicine Ethics Committee approval was taken (Date: 07.11.2023, Decision No: 2023/383) response of the patients

with lower limb ischemia accepted to the procedure with decreased walking distance measured by Doppler ultrasound were evaluated retrospectively.[11,12] Patients with puncture site infection, sepsis and patients with complication such as hematoma due to perforation were excluded from study. All procedures were carried out in accordance with the ethical rules and the principles of the Declaration of Helsinki.

Before the procedure, distal flows were measured and recorded with Doppler ultrasound which is evaluated by 5 year experienced radiology expert. (**Figure 1**). Patient positioned with supine position and main femoral artery, superficial femoral artery, popliteal artery , anterior tibial artery and posterior tibial artery evaluated respectively.

In addition, the vessel in which the patient's occlusive plaque was located and the endovascular method with which it was treated were noted.

After the patients were taken to the angiography suit, antegrade or retrograde access was made from the femoral artery according to the vessel where the stenosis-occlusion was located by an interventional radiologist with 10 year experience. In addition, brachial artery access was made in iliac occlusions. After the occlusion was passed with catheter and wire manipulation, balloon dilatation was applied. In cases accompanied by intimal flap or residual stenosis, stenting was performed. The procedure was terminated after control angiography images were obtained. The patients were kept under observation for 6 hours. After 6 hours, control USG and Doppler findings were recorded. If there were no complications, the patient was discharged. Demographic data of the patients were analyzed using descriptive statistics. Flow rates before and after the procedure were analyzed using the Student's t test. P value <0.05 was considered significant. SPSS ver. 24 (IBM corp. Armonk, NY, USA) program was used for statistical analysis.

RESULTS

The data of 9 patients with pre-procedure and Doppler findings were evaluated retrospectively. The demographic data of the patients are summarized in **Table 1**.

The average Rutherford category of the patients was 3.

Five patients had total superficial femoral artery (SFA) occlusion, three patients had total iliac artery occlusion, and one patient had distal abdominal aorta and both iliac branches occlusion.

Table 1. The demographic data of the patients

	Male	Female
Age	62.8	86.5
Smoking *	27.7	13
Comorbid disease		
Diabetes	3	0
Hypertension	2	2
COPD	1	1
Rutherford class	3	4

COPD: Chronic Obstructive Pulmonary Disease; *** :** Box per year

Regardless of the examination and method used, a significant increase was detected in distal blood flow measurements after the procedure. Doppler USG findings are summarized in **Table 2**.

While stenting was performed in 4 of the patients, only balloon dilatation was performed in the remaining 5 patients (**Figure 2**).

Table 2. Doppler findings of the patients

		Before procedure	After procedure	*P value
Pic-systolic velocity (cm/sec)	CFA	53.2	127.4	0.001
	SFA	15.2	75.8	
	Popliteal	16.8	65	
	ATA	10.4	45.4	
	ATP	10.7	30.5	
End-diastolic velocity(cm/sec)	CFA	11.4	21.4	0.001
	SFA	3.8	15.2	
	Popliteal	5.4	17.3	
	ATA	3.2	14.6	
	ATP	3.7	8.7	

*Student t test was used; CFA: Common femoral artery, SFA: Superficial femoral artery, ATA: Arteria tibialis anterior, ATP: Arteria tibialis posterior

DISCUSSION

In this study, we evaluated Doppler ultrasonography findings before and after endovascular treatment in patients with peripheral arterial disease (PAH). The findings show that endovascular interventions have significant positive effects on hemodynamic parameters. In most patients before treatment, arterial flow velocity and peripheral resistance values were significantly impaired due to disease progression. Significant improvements were observed in these values after treatment.

Doppler ultrasonography is an effective method to non-invasively evaluate changes in vessels in PAH. Previous studies have also shown similar findings; for example, Normahani et al.[13] (2021) reported an increase in flow velocity and improvement in vascular permeability after endovascular treatment. In line with this study, our findings also reveal that

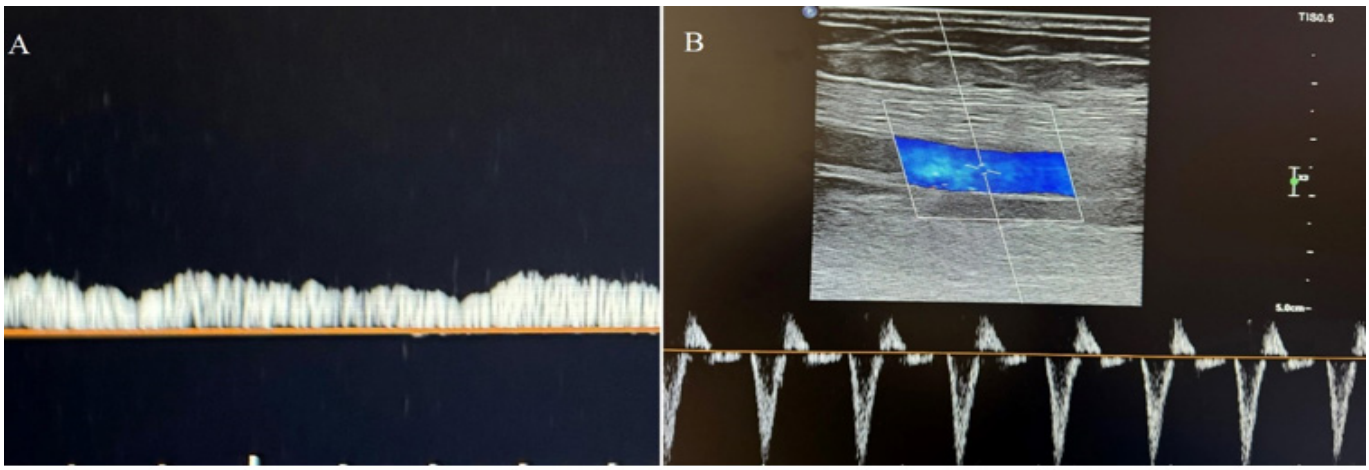

Figure 1. Monophasic flow pattern in the ipsilateral SFA due to iliac artery occlusion (A), and normal triphasic flow pattern is observed after endovascular treatment (B).

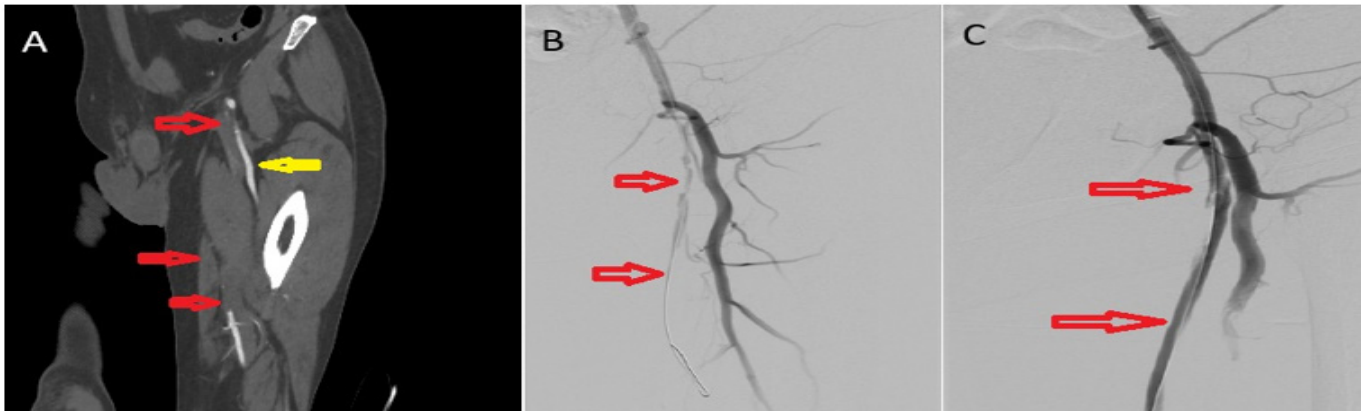

Figure 2. Occluded SFA (red arrow) and deep femoral artery (yellow arrow) without filling are observed in coronal reformatted tomography section (A), angiographic image of SFA occlusion (B), Flow is observed to be restored after balloon dilatation of the occlusion (red arrow) (C).

Doppler ultrasonography plays an important role in the treatment of PAH.

Endovascular treatment is a minimally invasive approach that positively affects the course of the disease. Lukacs et al.[14] (2024) reported significant increases in the quality of life and functional capacity of patients after treatment. Our study also supports the direct contribution of hemodynamic improvement to quality of life.

However, there are some limitations to this study. For example, the limited number of patients and the lack of long-term follow-up data may limit the generalizability of the results. In addition, the contribution of experienced experts is important in interpreting the data obtained with Doppler ultrasonography, therefore, the accuracy of the results can be further increased by standardizing the evaluations.

CONCLUSION

Doppler ultrasonography is an effective tool in monitoring hemodynamic changes in patients with PAH before and after endovascular treatment. Such studies are of great importance in optimizing treatment approaches and improving the clinical outcomes of patients. In the future, long-term follow-up studies with larger patient groups may better reveal the prognostic value of Doppler findings after endovascular treatment.

ETHICAL DECLARATIONS

Ethics Committee Approval

The study was approved by the Bolu Abant İzzet Baysal University Faculty of Medicine Ethics Committee (Date: 07.11.2023, Decision No: 2023/383).

Informed Consent

Because the study was designed retrospectively, no written informed consent form was obtained from patients.

Referee Evaluation Process

Externally peer-reviewed.

Conflict of Interest Statement

The authors have no conflicts of interest to declare.

Financial Disclosure

The authors declared that this study has received no financial support.

Author Contributions

All of the authors declare that they have all participated in the design, execution, and analysis of the paper, and that they have approved the final version.

REFERENCES

1. Sarıcaoğlu MC, Aytekin B, Yiğit G, Özen A, Zafer İşcan H. Endovascular balloon angioplasty for infrainguinal arterial occlusive disease: Efficacy analysis. *Turk Gogus Kalp Damar Cerrahisi Derg*. 2021;29(1):5-12.
2. Hirsch AT, Haskal ZJ, Hertzer NR, et al. ACC/AHA 2005 guidelines for the management of patients with peripheral arterial disease (lower extremity, renal, mesenteric, and abdominal aortic): executive summary: a collaborative report from the American association for vascular surgery/ society for vascular surgery, society for cardiovascular angiography and interventions, society for vascular medicine and biology, society of interventional radiology, and the ACC/AHA task force on practice guidelines (Writing committee to develop guidelines for the management of patients with peripheral arterial disease) endorsed by the American association of cardiovascular and pulmonary rehabilitation; 90 national heart, lung, and blood institute; society for vascular nursing; transatlantic inter-societyconsensus; and vascular disease foundation. *J Am Coll Cardiol*. 2006;47(6):1239-1312.
3. Tendera M, Aboyans V, Bartelink ML, et al. ESC Guidelines on the diagnosis and treatment of peripheral artery diseases. *Eur Heart J*. 2011;32(22):2851-2906.
4. De Sanctis JT. Percutaneous interventions for lower extremity peripheral vascular disease. *Am Fam Physician*. 2001;64(12):1965-1972.
5. Bendermacher BL, Teijink JA, Willigendael EM, et al. Symptomatic peripheral arterial disease: the value of a validated questionnaire and a clinical decision rule. *Br J Gen Pract*. 2006;56(533):932-937.
6. Goyen M, Ruehm SG, Debatin JF. MR angiography for assessment of peripheral vascular disease. *Radiol Clin North Am*. 2002;40(4):835-846.
7. Zheng ZJ, Sharrett AR, Chambless LE, et al. Associations of ankle-brachial index with clinical coronary heart disease, stroke and preclinical carotid and popliteal atherosclerosis: the Atherosclerosis Risk in Communities (ARIC) study. *Atherosclerosis*. 1997;131(1):115-125.
8. Crawford F, Welch K, Andras A, Chappell FM. Ankle brachial index for the diagnosis of lower limb peripheral arterial disease. *Cochrane Database Syst Rev*. 2016;9(9):CD010680.
9. Mills JL. Lower extremity arterial disease. In: Cronenwett JL, Johnston KW, editors. Rutherford's vascular surgery. Philadelphia: Elsevier. 2011;93(2):176.
10. Rowe VL, Lee W, Weaver FA, Etzioni D. Patterns of treatment for peripheral arterial disease in the United States: 1996-2005. *J Vasc Surg*. 2009;49(4): 910-917.
11. Fontaine R, Kim M, Kieny R. Surgical treatment of peripheral circulation disorders [in German] *Helv Chir Acta*. 1954;21(5-6):499-533.
12. Rutherford RB, Baker JD, Ernst C, et al. Recommended standards for reports dealing with lower extremity ischemia: revised version. *J Vasc Surg*. 1997;26(3):517-38. doi: 10.1016/s0741-5214(97)70045-4. Erratum in: *J Vasc Surg*. 2001; 33(4):805.

13. Normahani P, Khosravi S, Sounderajah V, Aslam M, Standfield NJ, Jaffer U. The effect of lower limb revascularization on flow, perfusion, and systemic endothelial function: a systematic review. *Angiology*. 2021;72(3):210-220.

14. Lukacs RA, Weisshaar LI, Tornyos D, Komocsi A. Comparing endovascular approaches in lower extremity artery disease: ınsights from a network meta-analysis. *J Clin Med*. 2024;13(4):1024

Journal of Radiology Medicine in

Original Article

Doi: 10.51271/JRM-0018

The comparison of the efficacy of 3D fast spoiled gradient echo sequence and steady state free precession sequence in imaging vascular compression in patients with trigeminal neuralgia

Mustafa Hızal, Ayşenur Buz Yaşar

Department of Radiology, Faculty of Medicine, Bolu Abant İzzet Baysal University, Bolu, Turkiye

Received: 029.09.2024 ◆ **Accepted**: 20.10.2024 ◆ **Published**: 30.10.2024

Cite this article: Hızal M, Buz Yaşar A. The comparison of the efficacy of 3D fast spoiled gradient echo sequence and steady state free precession sequence in imaging vascular compression in patients with trigeminal neuralgia. *J Radiol Med.* 2024;1(4):69-72.

Corresponding Author: Mustafa Hızal, hizal.mustafa@gmail.com

ABSTRACT

Aims: Trigeminal neuralgia (TN) is a condition characterized by sudden and intense pain in the face, affecting the fifth cranial nerve. While it can occur for various reasons, vascular compression is a well-known cause. Additionally, conditions such as tumors, arachnoid cysts, idiopathic inflammation, damage, or demyelination can result in TN, extending to the distal branches of the trigeminal nerve from the pons. We aimed to investigate the diagnostic efectiveness of post-contrast three-dimensional fast spoiled gradient echo images (3D-FSPGR) in addition to steady-state free precession (SSFP) images in the imaging of TN.

Methods: A total of 33 patients with a preliminary diagnosis of TN between May 2022 and October 2023 were investigated and five individuals were excluded. Among the remaining 28 patients, vascular compression was observed in only 14 patients. Trigeminal nerve thickness on both side, the distance between trigeminal nerve and superior cerebellar artery on both side, presence of vascular compression, level of the compression, presence or absence of displacement and atrophy were reported for each sequences. The findings and results were compared using independent sample T-test and paired T-test.

Results: The mean age of the patient group was calculated to be 56.29±4.5, while for the control group, it was 52.07±3.09. Trigeminal nerve thickness wasn't different between patient with or without vascular compression (p=0.874 for right side on SSFP, p=0.804 for left side on SSFP, p=0.667 for right side on 3D-FSPGR and 0.769 for left side on 3D-FSPGR). In 10 patients, unilateral compression of the trigeminal nerve was observed, while in 4 patients, it was bilateral. In the right trigeminal nerve, vascular compression was observed in SSFP images in 5 cases in the transitional zone, 2 cases in the nerve root entry zone, and 1 case distally. In 3D-FSPGR images, it was interpreted as being in the transitional zone in 4 cases, in the NR entry zone in 3 cases, and distally in 1 case.

Conclusion: Both SSFP and 3D-FSPGR images can provide comparable information regarding the spatial relationship between the trigeminal nerve and vascular structures. Contrast enhanced imaging allows us diferentiate the tumoral and infammatory demyelinating processes from vascular compression, we recommended to continue with SSFP images in cases where contrast enhanced 3D FSGPR images are inconclusive.

Keywords: Trigeminal neuralgia, three dimensional images, vascular compression

INTRODUCTION

Trigeminal neuralgia (TN) is a condition characterized by sudden and intense pain in the face, affecting the fifth cranial nerve, known as the trigeminal nerve.[1] Episodes of abrupt pain, lasting from seconds to minutes, can be triggered by factors such as chewing, speaking, exposure to cold air, wind, or laughter.[1,2] TN is often observed unilaterally. While it can develop for various reasons, vascular compression is a well-known cause.[3] Additionally, conditions such as tumors, arachnoid cysts, idiopathic inflammation, cervical discopathy, damage, or demyelination can result in TN, extending to the distal branches of the trigeminal nerve from the pons.[1-4] Under the International Classification of

Headache Disorders (ICHD-3) diagnostic criteria, TN is divided into classical, secondary, and idiopathic TN.[5] New diagnostic criteria are developed based on several clinical pieces of research.[5-8] Classical TN, caused by neurovascular compression, is the most common form of TN.[6,9] Secondary TN, which accounts for approximately 15% of cases, results from an external cause, such as a tumor or multiple sclerosis.[5,6,10]

We aimed to investigate the diagnostic effectiveness of post-contrast three-dimensional fast spoiled gradient echo images (3D-FSPGR) in addition to the commonly used and evaluated as standard method, balanced steady-state free precession (SSFP) images in the imaging of TN.

METHODS

Bolu Abant İzzet Baysal University Clinical Researches Ethics Committee approved the retrospective design of the study (Date: 07.11.2023, Decision No: 2023-379). And written informed consent was waived by them. A total of 33 patients referred to the radiology clinic for MRI with a preliminary diagnosis of TN between May 2022 and October 2023 were investigated and five individuals were excluded, with 4 patients lacking SSFP images and 1 patient with a mass causing TN. Among the remaining 28 patients, vascular compression was observed in only 14 patients. Trigeminal nerve thickness on both side, the distance between trigeminal nerve and superior cerebellar artery on both side, presence of vascular compression, level of the compression, presence or absence of displacement and atrophy were reported for each sequences. MR images were obtained with a 1.5 MRI system (GE Signa Explorer, USA). We obtained axial 3D FIESTA for SSFP and sagittal BRAVO for 3D-FSPGR. Paremeters for SSFP and 3D-FSPGR were, TR:7 ms, TE: 2.58 ms, matrix size: 300x288, NEX:4, slice thickness: 1 mm, spacing: 1 mm, FOV: 18x18 cm, bandwith 11kHz and TR:7 ms, TE: 3.03 ms, matrix size: 240x240, NEX:4, slice thickness: 1 mm, spacing: 1 mm, FOV: 25x25 cm, bandwith 11kHz, respectively. The findings and results of SSFP and 3D-FSPGR images of patients with and without vascular compression were compared using independent sample T-test and the measurements of the SSFP and 3D-FSPGR whole participants were compared using paired T-test.

RESULTS

The mean age of the patient group was calculated to be 56.29±4.5, while for the control group, it was 52.07±3.09. Of the patient group, 64.3 percent were female, while in the control group, 78.6 percent were female.

No statistically significant difference was found between the thickness of the right and left trigeminal nerves in both imaging sequences (p=0.286 and p=0.564, respectively). Additionally, the closest distance between the trigeminal nerve and vascular structure was similar in both sequences (p=0.375 and p=1) (**Table**). Also trigeminal nerve thickness wasn't different between patient with or without vascular compression (p=0.874 for right side on SSFP, p=0.804 for left side on SSFP, p=0.667 for right side on 3D-FSPGR and 0.769 for left side on 3D-FSPGR).

In 10 patients, unilateral compression of the trigeminal nerve was observed, while in 4 patients, it was bilateral. In the right trigeminal nerve, vascular compression was observed in SSFP images in 5 cases in the transitional zone, 2 cases in the nerve root entry zone, and 1 case distally (**Figure 1**). In 3D-FSPGR images, it was interpreted as being in the transitional zone in 4 cases, in the NR entry zone in 3 cases, and distally in 1 case. On the other hand, for the left trigeminal nerve, vascular compression was observed in both SSFP and 3D FSGPR images where the compression was observed in 5 cases in the nerve root entry zone, 3 cases in the distal zone, and 2 cases in the transitional zone (**Figure 2, 3, 4**).

Table. Trigeminal nerve thickness and the closest distance between nerve and superior cerebellar artery (SCA)

	SSFP images	3D-FSGPR images	p-value
All participants (n=28)			
Right trigeminal nerve thickness	2.92±0.6 mm	3.03±0.7 mm	p=0.286
Left trigeminal nerve thickness	2.94±0.7 mm	2.99±0.6 mm	p=0.564
The closest right trigeminal nerve and SCA distance	1.193±0.9 mm	1.136±0.9 mm	p=0.375
The closest left trigeminal nerve and SCA distance	1.05±0.9 mm	1.05±0.9 mm	p=1

SSFP: Steady-state free precession, 3D-FSGPR: Three-dimensional fast spoiled gradient echo images

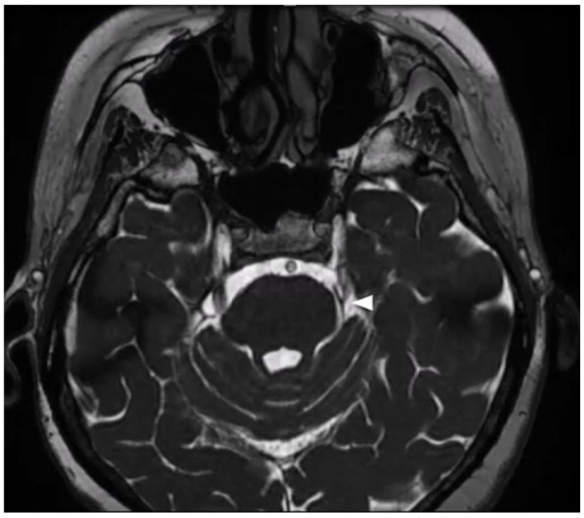

Figure 1. Axial SSFP image on the pons level. Vascular compression of left trigeminal nerve can be seen by left superior cerebellary artery (arrowhead)

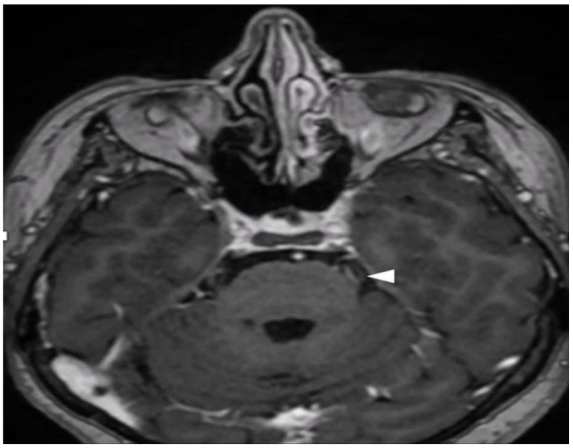

Figure 2. Axial contrast enhanced 3D-FSPGR image on the pons level. Vascular compression of left trigeminal nerve can be seen by left superior cerebellary artery (arrowhead)

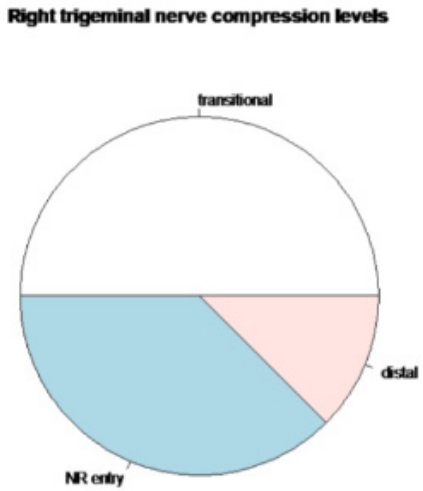

Figure 3. Pie chart of right trigeminal nerve compression levels

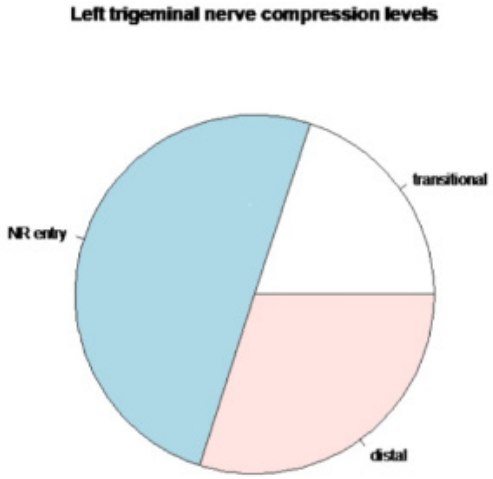

Figure 4. Pie chart of left trigeminal nerve compression levels

Displacement was present in the trigeminal nerve of only three patients, with two on the right side and one on the left for both imaging sequences. In SSFP sequence, atrophy was detected in six patients, with three on the right and three on the left. In 3D FSGPR images, atrophy was observed in five patients, with three on the right and two on the left.

DISCUSSION

In this study, we aimed to compare the efficacy of the 3D fast spoiled gradient echo (FSPGR) sequence and the SSFP sequence in visualizing vascular compression in patients with TN. TN is a neuropathic condition characterized by severe facial pain, often resulting from vascular compression of the trigeminal nerve. Precise imaging of neurovascular conflicts is crucial for both diagnostic and therapeutic purposes, especially when surgical intervention, such as microvascular decompression, is considered.

Both 3D-FSPGR and SSFP sequences provide valuable diagnostic information in detecting neurovascular compression; however, the SSFP sequence demonstrated superior clarity in identifying the compression site, especially in regions adjacent to the brainstem. This finding aligns with previous studies that emphasize the higher signal-to-noise ratio and contrast provided by SSFP sequences in neurovascular imaging.[11] SSFP is known for its ability to offer bright blood contrast, making it particularly useful in vascular imaging, which is consistent with our observations of its efficacy in depicting small vessels near the trigeminal nerve.

Conversely, the FSPGR sequence, while valuable for anatomical imaging, showed limitations in detecting smaller vessels, possibly due to its lower contrast resolution. These results are consistent with prior research indicating that FSPGR sequences, though widely used for anatomical imaging of the brain and nerves, may fall short in vascular detail when compared to SSFP. However, it is noteworthy that FSPGR sequences may still be preferable in patients where rapid acquisition time is necessary, or when motion artifacts are a concern.

The clinical implications of our findings are significant. The ability of the SSFP sequence to more clearly delineate vascular compression may lead to more accurate diagnoses and better surgical planning for patients with TN. As other studies have shown, accurate imaging is critical for determining the appropriate therapeutic approach, whether it be pharmacological treatment, percutaneous procedures, or microvascular decompression surgery.[12] The improved visualization of vascular compression provided by SSFP can potentially reduce the risk of misdiagnosis or unnecessary interventions.

However, our study does have limitations. The sample size was relatively small, and further studies with larger patient cohorts are necessary to validate our findings. Additionally, the imaging sequences were compared in a single institution using specific MRI machines and parameters, which may limit the generalization of the results to other settings or imaging systems. Future research could explore the application of these sequences across different institutions and with varying scanner configurations.

In conclusion, while both the 3D-FSPGR and SSFP sequences are useful in visualizing vascular compression in TN, SSFP demonstrates a higher diagnostic performance. Incorporating SSFP into routine imaging protocols for evaluating the relation between trigeminal nerve and vascular structure may enhance the accuracy of diagnosing neurovascular compression, thereby improving patient outcomes.

Since our results are similar in many measurements for both sequences, we suggest that either imaging sequence could be chosen without compromising the accuracy of trigeminal nerve thickness assessment. Additionally, the examination of the closest distance between the trigeminal nerve and superior cerebellar artery (SCA) in both imaging sequences showed no significant difference. This consistency supports the notion that both SSFP and 3D-FSPGR images can provide comparable information regarding the spatial relationship between the trigeminal nerve and vascular structures.

CONCLUSION

Our study highlights the reliability and consistency of both SSFP and 3D-FSPGR imaging sequences in assessing trigeminal nerve characteristics and vascular compression. Contrast enhanced imaging allows us differentiate the tumoral and inflammatory demyelinating procceses from vascular compression. Since the results are similar, we

recommended to continue with SSFP images in cases where contrast enhanced 3D-FSGPR images are inconclusive.

ETHICAL DECLARATIONS

Ethics Committee Approval

Bolu Abant İzzet Baysal University Clinical Researches Ethics Committee approved the retrospective design of the study (Date: 07.11.2023, Decision No: 2023-379).

Informed Consent

Because the study was designed retrospectively, no written informed consent form was obtained from patients.

Referee Evaluation Process

Externally peer-reviewed.

Conflict of Interest Statement

The authors have no conflicts of interest to declare.

Financial Disclosure

The authors declared that this study has received no financial support.

Author Contributions

All of the authors declare that they have all participated in the design, execution, and analysis of the paper, and that they have approved the final version.

REFERENCES

1. Haller S, Etienne L, Kövari E, Varoquaux AD, Urbach H, Becker M. Imaging of neurovascular compression syndromes: trigeminal neuralgia, hemifacial spasm, vestibular paroxysmia, and glossopharyngeal neuralgia. *AJNR. Am J Neuroradiol*. 2016;37(8):1384-1392.
2. Anwar H, Ramya Krishna M, Sadiq S, et al. A study to evaluate neurovascular conflict of trigeminal nerve in trigeminal neuralgia patients with the help of 1.5 T MR imaging. *Egypt J Radiol Nucl Med*. 2022;53(1):66.
3. Hughes MA, Frederickson AM, Branstetter BF, Zhu X, Sekula RF. MRI of the trigeminal nerve in patients with trigeminal neuralgia secondary to vascular compression. *AJR. Am J Roentgenol*. 2016;206(3):595-600.
4. Turk Boru U, Boluk C, Ozdemir A, et al. Cervical discopathy in idiopathic trigeminal neuralgia: more than coincidence? *Adv Spine J*. 2021;40(1):53-64.
5. Headache Classification Committee Of The International Headache Society (IHS): The International Classification Of Headache Disorders, 3rd Edition. *Cephalalgia*. 2018;38:1-211.
6. Cruccu G, Finnerup NB, Jensen TS, et al. Trigeminal neuralgia: new classification and diagnostic grading for practice and research. *J Neurol*. 2016;87(2):220-228.
7. Antonini G, Di Pasquale A, Cruccu G, et al. Magnetic resonance imaging contribution for diagnosing symptomatic neurovascular contact in classical trigeminal neuralgia: a blinded case-control study and meta-analysis. *Pain*. 2014;155(8):1464-1471.
8. Jannetta PJ. Arterial compression of the trigeminal nerve at the pons in patients with trigeminal neuralgia. *J Neurosurg*. 1967;26(1):159-162.
9. Miller J, Acar F, Hamilton B, Burchiel K. Preoperative visualization of neurovascular anatomy in trigeminal neuralgia. *J Neurosurg*. 2008; 108(3):477-482.
10. Dandy WE. Concerning the cause of trigeminal neuralgia. *Am J Surg*. 1934;24(2):447-455.
11. Müller S, Khadhraoui E, Khanafer et al. Differentiation of arterial and venous neurovascular conflicts estimates the clinical outcome after microvascular decompression in trigeminal neuralgia. *BMC Neurol*. 2020;20(1):279.
12. Lemos L, Alegria C, Oliveira J, Machado A, Oliveira P, Almeida A. Pharmacological versus microvascular decompression approaches for the treatment of trigeminal neuralgia: clinical outcomes and direct costs. *J Pain Res*. 2011;4:233-244.

Journal of Radiology Medicine in

Original Article

Doi: 10.51271/JRM-0019

Peripheral arterial disease: a single center experience

Muhammed Karadeniz, Çağlar Alp

Department of Cardiology, Faculty of Medicine, Kırıkkale University, Kırıkkale, Turkiye

Received: 07.10.2024 ◆ **Accepted**: 28.10.2024 ◆ **Published**: 30.10.2024

Cite this article: Karadeniz M, Alp Ç. Peripheral arterial disease: a single center experience. *J Radiol Med.* 2024;1(4):73-76.

Corresponding Author: Muhammed Karadeniz, drkaradeniz36@gmail.com

ABSTRACT

Aims: Angiography and interventional treatment modalities in peripheral arterial disease have recently been widely used because they are easier to perform and more comfortable than surgical treatment. Revascularization is the most effective treatment method in cases such as critical leg ischemia in this disease where pharmacological agents are also widely used. In this study, we aimed to investigate interventional treatment methods in peripheral arterial disease in our center.

Methods: Patients who underwent peripheral angiography or endovascular intervention in the Cardiology Clinic of Kırıkkale University Medical Faculty Hospital between March 2020 and June 2024 were retrospectively reviewed.

Results: A total of 55 patients, including 10 women and 45 men, were included in the study. The mean age of the patients included in the study was 64 years. Of the angiographic procedures, 46 were performed in the lower extremity, 6 in the upper extremity and 3 in the renal arteries. Endovascular treatment were performed in 26 of them. Of the endovascular treatment, 11 were balloon angioplasty and 15 were stent implantation. In 5 patients, peripheral bypass was decided.

Conclusion: Interventional treatment of peripheral arterial disease is increasingly and successfully performed in our center.

Keywords: Peripheral arterial disease, endovascular intervention, balloon angioplasty, stent implantation

INTRODUCTION

Peripheral arterial disease (PAD) is a disease characterized by narrowing or occlusion of the arterial circulation, especially in the lower extremities, due to atherosclerosis. The prevalence of PAD increases with age and has been reported to be between 3-7% under the age of 60 years, 20% in men and 15% in women over the age of 65 years.[1] In a multicenter study called "careful" conducted in Turkey in 2010 to investigate the prevalence of peripheral artery disease, patients aged 50-69 years with at least one cardiovascular risk factor and all patients over the age of 70 years were included in the study. The diagnosis of PAD was made by measuring the ankle-brachial index (ABI). As a result of the study, the prevalence of PAD was found to be 20% in all age groups and 30% in patients over 70 years of age.[2] Advanced age, male gender, smoking status, and diseases such as diabetes, hypertension, hyperlipidemia and metabolic syndrome have been reported as risk factors for PAD.[3] Especially in diabetic patients, symptoms are recognized late due to peripheral neuropathy and complications such as limb amputation are more common.

Although 1/3-1/2 of patients are asymptomatic, the most common symptom is leg pain (claudication intermittent), which initially occurs with exertion, but as the severity of the stenosis increases, this pain starts to occur at rest. In advanced cases, sores appear on the foot. ABI measurement is widely used as a non-invasive screening method for the diagnosis of peripheral arterial disease. ABI between 1.0-1.3 is considered normal. An ABI ≤0.9 is diagnostic for PAD.[4] This value may be abnormally high due to highly calcified arteries, which may be present in diabetes and renal diseases.[4] Although peripheral arterial surgery is still performed in the treatment of PAD, endovascular interventional treatments are preferred in most cases with the development of device and balloon-stent technology.[5,6] PAD, which causes a significant increase in comorbidity and mortality when left untreated, is an important disease to be diagnosed early. Easy diagnosis with ABI and treatment with interventional and surgical methods may prevent serious complications such as amputation.[6]

In this study, we retrospectively analyzed the patients who underwent peripheral angiography and peripheral angioplasty in appropriate patients in our clinic.

METHODS

This is an observational study in which patients who underwent peripheral angiography and endovascular intervention for

peripheral arterial disease were retrospectively analyzed. Ethics committee approval was obtained from Kırıkkale University Non-interventional Clinical Researches Ethics Committee (Date: 17.04.2024, Decision No: 2024.04.12). All procedures were carried out in accordance with the ethical rules and the principles of the Declaration of Helsinki. Patients who were hospitalized for peripheral angiography or endovascular intervention in the Cardiology Clinic of Kırıkkale University Medical Faculty Hospital between March 2020 and June 2024 were retrospectively reviewed. Peripheral angiography was performed in patients with foot pain and ABI≤0.9, and renal angiography was performed in those with resistant hypertension. Inclusion criteria: age older than 18 years, undergoing angiography or endovascular intervention on iliac, femoral, popliteal, tibial, peroneal, carotid, vertebral, subclavian, brachial, renal and mesenteric arteries.

Medical history, demographic characteristics, laboratory parameters, and in-hospital adverse events such as post-procedural death, myocardial infarction, cerebrovascular accident, contrast nephropathy, and access site complications were obtained from hospital records. The characteristics of the angiography, types of lesions, type of balloon and stent used in endovascular intervention, success and complications of the procedure were recorded. The success of the procedure was defined as antegrade flow after balloon dilatation or stenting.

Statistical Analysis

Statistical analysis of the data was performed using the Statistical Package for the Social Sciences for Windows (SPSS Inc., Chicago, Illinois, USA) 21.0 program. Descriptive statistics were expressed as mean±standard deviation for continuous variables and number of cases and (%) for categorical variables. The Kolmogorov-Smirnov test was used to determine whether the distributions of continuous variables were normal. Continuous variables with normal distribution were compared by Student-t test and continuous variables without normal distribution were compared by Mann-Whitney-U test. Chi-square test or Fischer Exact test was used to compare categorical variables. The statistical significance level of the obtained data was interpreted with "p" value. $p<0.05$ values were considered statistically significant.

RESULTS

A total of 57 peripheral angiography procedures between March 2020 and June 2024 were retrospectively analyzed. Peripheral angiography was performed on the following patients; for extremities; patients with claudication, foot wounds, ABI ≤0.9 and patients with lesions detected on noninvasive imaging methods, for renal arteries; patients with resistant hypertension. A total of 55 patients, including 10 women and 45 men, were included in the study. The mean age of the patients included in the study was 64 years. Of the angiographic procedures, 46 were performed in the lower extremity, 6 in the upper extremity and 3 in the renal arteries (**Figure 1**). Demographic and clinical characteristics of the patients are given in **Table 1**.

Endovascular intervention was performed in 26 patients, 15 of whom also underwent stent implantation. Balloon angioplasty was performed on 11 patients. Heparin and clopidogrel were administered to patients before endovascular treatment. The mean age of patients undergoing interventional procedures was 64 years, in line with the study population, and 19 (73%) were male. Peripheral artery endovascular treatment was performed in the iliac arteries, femoral arteries, tibialis anterior/posterior and peroneal arteries. Balloon angioplasty was performed in lesions without total occlusion or with short total occlusion (**Figure 2**). In patients with dissection after balloon angioplasty, a balloon expanding stent was deployed in the iliac artery and a self-expanding stent was deployed in the femoral artery (**Figure 3, 4**). Stent deployment was not performed in the tibialis anterior/posterior and peroneal arteries. The balloons and stents used during endovascular procedures were not drug-eluting. Rupture occurred during intervention in the superficial femoral artery in 2 patients, but the rupture was self-limiting and surgery was not required.

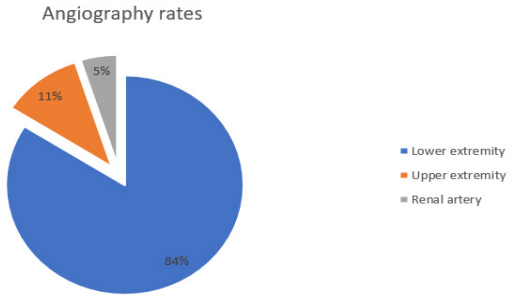

Figure 1. Distribution of peripheral angiographic procedures

Table 1. Demographic and clinical characteristics of the PAD patients

Demographic characteristics	**n (total=55)**	**%**
Age (year)	64±10	
Gender (male)	45	82.1
Diabetes	32	56.1
Hypertension	38	66.7
Hyperlipidemia	42	73.7
Cigarette	25	48.1
History of cerebrovascular accident	5	8.9
Coronary artery disease	15	26.8
Types of peripheral angiography		
Subclavian artery	6	10.7
Iliac artery	16	28.6
Superficial femoral artery	23	41.1
Tibialis anterior/posterior and peroneal artery	7	12.5
Renal artery	3	5.4
Angioplasty data		
Medical treatment	25	44.6
Balloon angioplasty	11	19.6
Stent	15	26.8
Surgery	5	8.9

PAD: Eripheral arterial disease

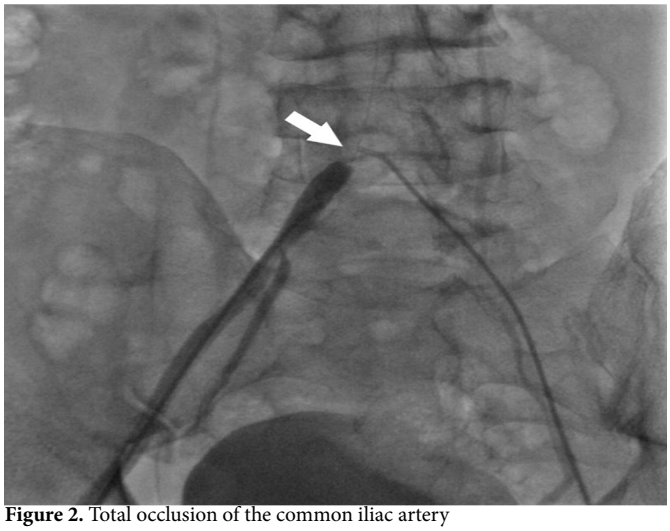

Figure 2. Total occlusion of the common iliac artery

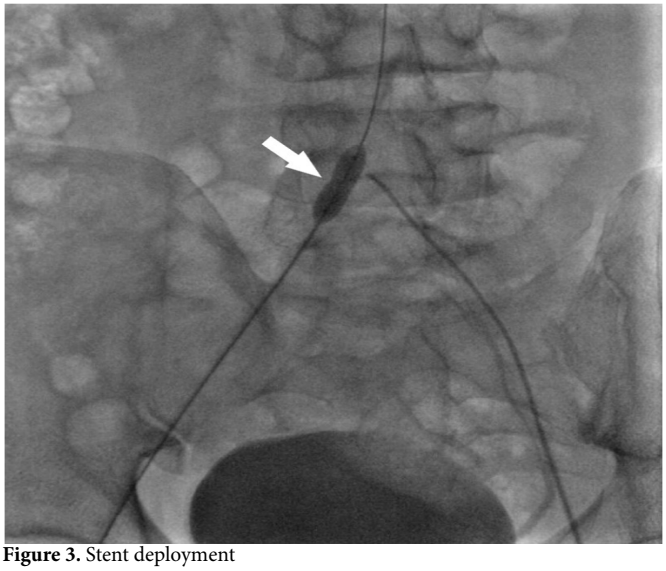

Figure 3. Stent deployment

Figure 4. Revascularization of the common iliac artery

Diabetes, one of the most important risk factors for peripheral arterial disease, was present in 32 patients (56.1%). Hyperlipidemia was also the most common risk factor (73.7%). The mean HbA1c of the study population was 9.8%.

Table 2. Laboratory findings of the PAD patients

Laboratory findings	mean±SD
Systolic blood pressure (mmHg)	132±23
Diastolic blood pressure (mmHg)	82±15
Pulse	75±11
White blood cell (10^3/μL)	9.0±2.8
Hemoglobin (g/dl)	13.6±1.7
Platelet ($\times10^9$/L)	271±80
Glucose (mg/dl)	140±54
HbA1c (%)	9.8±2.1
Creatinine (mg/dl)	1.08±0.8
Total cholesterol (mg/dl)	171±44
LDL cholesterol (mg/dl)	91±20
HDL cholesterol (mg/dl)	45±13
Triglycerides (mg/dl)	184±48

PAD: Peripheral arterial disease, SD: Standard deviation

DISCUSSION

Peripheral arterial disease is a condition that should be kept in mind together with coronary artery disease, especially in patients with high cardiovascular risk factors, as it can be asymptomatic. If left untreated, it can lead to lower limb amputations and upper limb pain and limitation of mobility. The diagnosis of PAD can be made by non-invasive methods such as ABI. In the treatment of PAD, peripheral balloons, especially drug-coated peripheral balloons and stents, which have been developed in parallel with technological developments in the last decade, have significantly reduced restenosis rates. When we look at the rates of peripheral angiography and endovascular intervention in our center, percutaneous transluminal angioplasty was performed in almost half of the patients. In the past, most patients with PAD were treated medically or surgically, but recently, with the development and widespread use of imaging methods and endovascular devices, endovascular intervention can be performed in a significant proportion of patients. Compared to surgery, endovascular interventions are more preferred today because they are more comfortable, cause less bleeding and infection, allow for repeated interventions and cause fewer in-hospital events.

The results of endovascular interventions in large diameter arteries such as the subclavian, iliac and femoral arteries are encouraging. In the resilient study, primary implantation of a self-expanding nitinol stent in medium-length lesions in the superficial femoral artery and proximal popliteal artery was associated with better acute angiographic results and improved patency compared with balloon angioplasty.[7] In a study of 775 patients comparing paclitaxel-eluting stents with bare metal stents in superficial femoral and proximal popliteal artery lesions, there was no difference in all-cause mortality between the two groups, but the incidence of primary sustained clinical improvement was higher with drug eluting stents than with bare metal stents.[8] A meta-analysis compared old balloon angioplasty with drug-coated balloon angioplasty and showed that drug-coated angioplasty significantly reduced late lumen loss, dual restenosis and target lesion revascularization in the treatment of femoropopliteal disease.[9] It should be kept in mind that stent implantation may carry some risks because the femoropopliteal region is a region with active joint movements. Drug-coated balloon angioplasty is currently considered the most appropriate treatment option. In case of dissection after balloon, self-expanding stent may be considered. Restenosis rates are high with standard balloon treatment in the tibialis anterior, tibialis posterior and peroneal arteries below the knee. In a study by Fernandez et al.[10] in patients with critical leg ischemia, the one-year re-intervention rate after bare balloon treatment was found to be 50%. Regarding drug-eluting balloons, while some studies showed no difference compared to standard balloons, a study by Gür et al.[11] found that drug-eluting balloons were superior to bare balloons in terms of 12-month patency rates and amputation rates. There is no consensus in studies on endovascular intervention in the arteries below the knee. For lesions in this region, treatment modalities such as pharmacologic therapy, smoking cessation and exercise can be applied. However, endovascular intervention is recommended if the patient has critical foot ischemia or a foot wound.[12]

Limitations

Since it was a single center, the number of patients was small, and since it was a retrospective study, post-discharge follow-up data were not available.

CONCLUSION

As a result, PAD is a disease whose prevalence increases with age in our country as in the whole world. Interventional treatment methods in PAD have recently been applied more frequently than surgical methods with improved materials and increasing experience.

ETHICAL DECLARATIONS

Ethics Committee Approval

The study was initiated with the approval of the Kırıkkale University Non-interventional Clinical Researches Ethics Committee (Date: 17.04.2024, Decision No: 2024.04.12).

Informed Consent

Because the study was designed retrospectively, no written informed consent form was obtained from patients.

Referee Evaluation Process

Externally peer-reviewed.

Conflict of Interest Statement

The authors have no conflicts of interest to declare.

Financial Disclosure

The authors declared that this study has received no financial support.

Author Contributions

All of the authors declare that they have all participated in the design, execution, and analysis of the paper, and that they have approved the final version.

REFERENCES

1. Welten GM, Schouten O, Chonchol M, et al. Prognosis of patients with peripheral arterial disease. *J Cardiovasc Surg (Torino)*. 2009;50(1):109-121.
2. Bozkurt AK, Tasci,I, Tabak O, Gumus M, Kaplan Y. Peripheral artery disease assessed by ankle-brachial index in patients with established cardiovascular disease or at least one risk factor for atherothrombosis-CAREFUL Study: a national, multi-center, cross-sectional observational study. *BMC Cardiovasc Disord*. 2011;11(4):1-10.
3. Shammas NW. Epidemiology, classification, and modifiable risk factors of peripheral arterial disease. *Vasc Health Risk Manag*. 2007;3(2):229-234.
4. Ankle Brachial Index Collaboration, Fowkes FG, Murray GD, et al. Ankle brachial index combined with Framingham Risk Score to predict cardiovascular events and mortality: a meta-analysis. *JAMA*. 2008;300(2): 197-220.
5. Hirsch AT, Haskal ZJ, Hertzer NR, et al. ACC/AHA 2005 guidelines for the management of patients with peripheral arterial disease (lower extremity, renal, mesenteric, and abdominal aortic): executive summary a collaborative report from the American Association for Vascular Surgery/ Society for Vascular Surgery, Society for Cardiovascular Angiography and Interventions, Society for Vascular Medicine and Biology, Society of Interventional Radiology, and the ACC/AHA Task Force on Practice Guidelines (Writing Committee to Develop Guidelines for the Management of Patients With Peripheral Arterial Disease) endorsed by the American Association of Cardiovascular and Pulmonary Rehabilitation; National Heart, Lung, and Blood Institute; Society for Vascular Nursing; TransAtlantic Inter-Society Consensus; and Vascular Disease Foundation. *J Am Coll Cardiol*. 2006;47(6):1239-1312.
6. Rooke TW, Hirsch AT, Misra S, et al. Management of patients with peripheral artery disease (compilation of 2005 and 2011 ACCF/AHA Guideline Recommendations): a report of the American College of Cardiology Foundation/American Heart Association Task Force on Practice Guidelines. *J Am Coll Cardiol*. 2013;61(14):1555-1570.
7. Laird JR, Katzen BT, Scheinert D, et al. Nitinol stent implantation versus balloon angioplasty for lesions in the superficial femoral artery and proximal popliteal artery: twelve-month results from the RESILIENT randomized trial. *Circ Cardiovasc Interv*. 2010;3(3):267-276.
8. Gouëffic Y, Torsello G, Zeller T, et al. Efficacy of a drug-eluting stent versus bare metal stents for symptomatic femoropopliteal peripheral artery disease: primary results of the EMINENT randomized trial. *Circulation*. 2022;146(21):1564-1576.
9. Caradu C, Lakhlifi E, Colacchio EC, et al. Systematic review and updated meta-analysis of the use of drug-coated balloon angioplasty versus plain old balloon angioplasty for femoropopliteal arterial disease. *J Vasc Surg*. 2019;70(3):981-995.e10.
10. Fernandez N, McEnaney R, Marone LK, et al. Predictors of failure and success of tibial interventions for critical limb ischemia. *J Vasc Surg*. 2010; 52(4):834-842.
11. Gür Ö, Donbaloğlu MO, Gürkan S. Comparison of drug eluting balloon versus standard balloon results in patients with below knee peripheral artery disease. *Düzce Tıp Fak Derg/Duzce Med J*. 2018;20(3):73-76.
12. Conrad MF, Kang J, Cambria RP, et al. Infrapopliteal balloon angioplasty for the treatment of chronic occlusive disease. *J Vasc Surg*. 2009;50(4):799-805.

Journal of Radiology Medicine in

Review

Doi: 10.51271/JRM-0020

Applications of artificial intelligence in age estimation: a review

Abdulkadir Sancı, Burak Kaya

Forensic Medicine Specialist, Artvin Forensic Medicine Branch Office, Artvin, Turkiye

Received: 10.09.2024 ◆ **Accepted**: 04.10.2024 ◆ **Published**: 30.10.2024

Cite this article: Sancı A, Kaya B. Applications of artificial intelligence in age estimation: a review. *J Radiol Med*. 2024;1(4):77-83.

Corresponding Author: Abdulkadir Sancı, akadirsanci@gmail.com

ABSTRACT

Age estimation is a legally significant issue, particularly in underdeveloped and developing countries, due to factors such as inadequate civil registration systems and irregular migration. While various techniques are employed for age estimation using traditional methods, it is known that factors including age, gender, chronic illness, race, and geographical region can result in discrepancies between skeletal age and chronological age. This complicates the process of achieving accurate age estimation. This review aims to discuss recent research on artificial intelligence applications in light of current literature. Artificial intelligence and machine learning (ML) have enabled machines to acquire human-like capabilities in thinking, learning, problem solving, and decision making, leading to significant progress in achieving faster and accurate results. In the field of forensic medicine, methods such as linear discriminant analysis, K-Nearest Neighbors, support vector machines, random forests, and artificial neural networks have been employed to classify data and conduct studies on age estimation. In the research, age estimation was made by focusing especially on the carpal bones, ossification centers, middle phalanx of the hand, third metacarpal, radius and ulna regions. Additionally, facial angles and width obtained through tomographic examinations, as well as measurements of the calcaneus and cuboid bones, panoramic dental radiographs, volumetric analysis of teeth and pulp using cone beam computed tomography, and analysis of bloodstains on microRNAs, have been analyzed for their distribution across different age. The results demonstrate that artificial intelligence applications can be utilized in age estimation with a high accuracy rate (85-95%). Age estimation using artificial intelligence enhances data-driven decision-making processes, improves the quality of services, and contributes to societal benefit. Therefore, we believe that incorporating artificial intelligence applications alongside traditional methods in age estimation will yield more meaningful outcomes.

Keywords: Age estimation, artificial intelligence, radiology, forensic medicine

INTRODUCTION

The term "identity" refers to all characteristics that are effective in recognizing, identifying, and distinguishing an individual from others. The process of identifying these characteristics in both living individuals and postmortem examinations is referred to as "identity verification." Identity verification is a necessary practice for both living individuals and deceased persons for various reasons. In contemporary times, the identification of individuals has transcended being merely a personal or societal issue, gaining international significance. One of the critical elements of identification is the determination of a person's age. Physical characteristics such as age, gender, height, weight, hair type, skin tone, eye color, fingerprints, bone structure, and dental structure are among the key aspects of identification.[1]

THE IMPORTANCE OF AGE ESTIMATION

It is a fundamental human right for individuals to know their true age. Age estimation serves as an important document that completes and validates an individual's identity characteristics. For instance, it has been observed that the Romans used the eruption of the first permanent molars in the mouth to determine whether a person was of military age, indicating the use of teeth in age estimation.[2]

For individuals whose birth dates have not been reliably recorded, forensic age estimation is required. Today, forensic age estimation is a significant area of evaluation, particularly in civil and criminal law. The reasons for requesting forensic age estimation can vary between countries and regions. In Turkey, the primary reason for this need is the late registration of children in the population registry, especially in rural

areas. For individuals whose population registry information is questioned, forensic age estimation is also requested in legal processes concerning criminal law, as well as for living individuals in situations such as school enrollment, job applications, marriage, and military service.[3] In recent years, migration has become a significant global issue. The intense migration and the lack of official documents among migrants have necessitated age estimation for identity verification, making this a global concern. Age estimation has gained importance in migrants in terms of verifying their identity, accessing social services, and in potential legal processes and judicial proceedings if they commit or are subjected to crimes.

In forensic medicine, age estimation, whether for living individuals in the antemortem period or for deceased individuals in postmortem examinations, holds great importance in both criminal and civil law.[4] As in the past, today, the determination of an individual's true age is crucial in determining their criminal and legal responsibility, their capacity to comprehend the legal meaning and consequences of their actions, their psychological protection in cases of sexual assault, the determination of the age of suspects in criminal acts, as well as in situations such as school enrollment, entering public service, retirement, and obtaining a driver's license.[5] Additionally, forensic authorities request age estimation for unidentified individuals or infant corpses.

In criminal law, age groups in Turkey are categorized into three groups: 0-12, 12-15, and 15-18 years. Similar age groupings are made in other countries as well. In Germany, the age groups are 0-14, 14-18, and 18-21 years; in England, 0-7, 7-14, and 14-17 years; in France, 0-13, 13-16, and 16-18 years; and in Russia, 0-14, 14-18, and 18-20 years. Switzerland categorizes age groups into four groups: 0-7, 7-15, 15-18, and 18-25 years. In Turkey, discrepancies between the actual age and the age recorded in the population registry are more frequently encountered at critical ages from a legal perspective, such as 12, 15, 18, and 21 years. Many laws in Turkey define the age factor. Additionally, the Population Law specifies how population records should be corrected and who is authorized to request these corrections. Article 7 of the Civil Code, under the heading of proof with official documents, states that official registers and records are deemed to validate the accuracy of the information they document. Unless another regulation is specified in the laws, no specific formal requirement is needed to prove the inaccuracy of these documents. It is emphasized that if an individual was born in a hospital or has an official birth certificate, the court should give priority to these documents. In such cases, a medical report is not required for age estimation.[6]

In our country, discrepancies between the declared age and the actual age often arise due to late population registrations or the use of the identity information of a deceased child for a newborn. Furthermore, issues such as concealing age information or using false identities can lead to various problems in situations requiring age-based restrictions, such as migration, inheritance, legal cases, sports, and retirement.[7]

METHODS USED IN AGE ESTIMATION

Age estimation methods are categorized into three main categories: radiological, morphological, and histological. Among these, radiological and morphological methods are the most frequently used. The criteria evaluated in these methods cover a broad spectrum. Key criteria include height, weight, signs of adolescence, hair, skin changes, eye changes, psychological state, teeth, and bone development. Physiological and pathological factors affecting an individual's development, physical findings such as height, weight, dental development, signs of puberty, psychological and mental development, and radiological assessments of ossification between the epiphysis and metaphysis of bones and the timing of physiological calcification of bones are examined.[3]

In radiological examinations, primary atlases prepared according to the standards of Western societies are used for comparison. These include the Greulich and Pyle (G-P) atlas, Tanner-Whitehouse (T-W) scoring, and the V. Gilsanz-O. Ratib atlas. Radiological analyses assess whether the epiphyseal lines of bones have closed, changes at the vertebral and sternal ends of the ribs, the calcification states of the sternum and sacrum, the formation of osteophytes due to senility, and changes in the internal structure of bone tissue (e.g., osteoporosis, thinning of the trabeculae in the medulla). These methods are among the most commonly used and reliable techniques for age estimation. Radiological methods such as the formation and development of growth plates in bones, the evaluation of epiphyseal and diaphyseal lines, and the determination of ossification points play a significant role in clinical applications for age estimation and provide results closest to reality.[9]

For radiological examinations, hand-wrist radiographs are considered for bone development stages under the age of 12, while hand finger and metacarpal bones, lower epiphysis radiographs of the radius and ulna, anterior and lateral elbow radiographs, shoulder radiographs showing the humerus neck, and unilateral pelvis radiographs including the iliac upper and ischial lower edges are used for age estimation between 12-22 years. Sacrum and lateral coccyx radiographs are examined for ages 23-40, lateral sternum radiographs around age 40, and anterior chest radiographs between 45-50 years.[1] Some national studies have used clavicle medial epiphysis for computed tomography staging to determine age between 19-21 years,[10] while other studies have used tomography to examine the degree of sacral vertebral fusion,[11] bimastoid width measurements,[12] and face-ear distance measurements[13] for age estimation.

In forensic dentistry, archaeology, and forensic medicine, various methods are being researched to determine the age of skeletal remains or unidentified bodies with minimal margin of error. Advances in forensic odontology have contributed to the increase in dental examinations and the acquisition of more accurate results. Teeth are often used for age estimation in identification. Due to their hard structure and low metabolic rate, it is suggested that the data obtained from dental development provides more accurate results than other structures in the organism.[14]

The evaluation of dental tissue has long been considered a reliable tool for age estimation, and techniques applied to these tissues have been widely used by forensic dentists, forensic pathologists, and anthropologists. The scientific rationale for dental tissue evaluation in age estimation is based on three criteria: 1. Formation and growth changes of teeth, 2. Post-formation changes, 3. Biochemical changes.

The formation and growth of teeth encompass the morphological development of the crown, root, and apex points of the tooth, including the emergence, eruption, and progression stages. An important advantage of age estimation using dental formation and growth techniques in forensic dentistry is that they are non-invasive and can be easily evaluated through inspection and radiographic examination. Once growth in teeth and bones ceases, forensic dentists employ techniques involving the biochemical changes or post-formation changes of the teeth for age estimation: aspartic acid racemization and Carbon-14 age testing. Both are expensive and time-consuming laboratory techniques that examine tooth structure.[15]

One of the age estimation methods is the histological method. Recent studies in this field have focused on histomorphological and histochemical techniques. These methods estimate age by examining characteristics such as bone structure, muscle fiber types, and myosin heavy chains. Additionally, examining cell proliferation using the AgNOR staining method on abdominal skin samples from age groups has emerged as an alternative approach to age estimation. The clinical applicability of these methods provides significant clarity in cases where definitive age estimation is not possible. However, because new methods have not yet been standardized to provide consistent and reliable results, existing methods still play an important role.[9]

Another important aspect of age estimation is identifying endocrine diseases that affect growth and development and evaluating the extent of their impact. Various metabolic, hormonal, and genetic diseases that can lead to early or delayed bone development include obesity, diabetes, hypothyroidism, growth hormone deficiency, celiac disease, ulcerative colitis, nephrotic syndrome, goiter, hypercalcemia, phenylketonuria, Down syndrome, Turner syndrome, and Angelman syndrome. Additionally, factors such as gender, race, socioeconomic status, and trauma can also influence this condition (**Table**).[16] There is very limited national and international literature on the impact of growth and development-affecting diseases on age estimation, particularly in children with diabetes, obese children, pregnant or previously pregnant children, genetic malformations, and other growth-impairing conditions. In studies on age assessment in diabetic children, Dost and colleagues reported in 2010 that in their study of bone development in 1788 German and Austrian children diagnosed with type 1 diabetes, the bone ages of diabetic children and adolescents were significantly delayed, with the difference ranging from 0.27 to 1.1 years. Those over 16 years old showed more pronounced bone age retardation compared to other cases. It was also reported that the delay in bone age in males was more significant than in females. Bone age was found to be significantly delayed in individuals with high HbA1c levels and poor glycemic control from the onset of diabetes to the determination of bone age.[17] It has been reported that all these traditional methods commonly used in forensic age estimation may result in inaccuracies due to factors such as the lack of data in new research and statistical analyses, individual differences, and environmental factors. This situation complicates the achievement of accurate age estimation. However, with the advancement of technology, the use of artificial intelligence (AI) applications has increased; studies have reported that higher accuracy results can be achieved in forensic age estimation through artificial intelligence.

Table 1. Causes of discrepancy between bone age and chronological age 2

Bone age <chronological age	Bone age >chronological age
Hypothyroidism (congenital & acquired)	Precocious puberty
Growth hormone deficiency	Premature adrenarche
Panhypopituitarism	Congenital adrenal hyperplasia
Hypogonadism	Hyperthyroidism
Constitutional growth delay	Constitutional tall stature
Rickets	Obesity
Corticosteroid excess syndromes (Turner, Down, Klinefelter, Silver-Russell)	Overgrowth syndromes (Sotos, Beckwith-Wiedemann syndrome)
Malnutrition (primary or secondary to chronic disease)	

ARTIFICIAL INTELLIGENCE AND COMMONLY USED METHODS IN DATA ANALYSIS

AI can achieve faster and more accurate results than humans in data analysis, identifying connections between data, and making predictions. AI algorithms, often working with large datasets, can effectively analyze biological features for age estimation. For example, it is possible to estimate age through the analysis of radiological images of bones and teeth.[18]

The primary function of AI is to classify uploaded data and develop algorithms that evaluate the relationships between these data. Among these classification techniques is Linear Discriminant Analysis, which reduces a two-variable dataset to a single variable and draws a linear boundary between classes (**Figure 1**). Other classifiers, such as K-Nearest Neighbors (KNN), Support Vector Machines (SVM), Random Forest, and Bagging, have the ability to create non-linear boundaries between class samples.

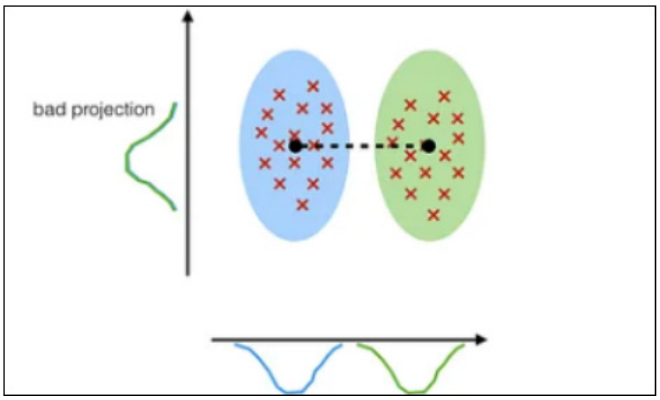

Figure 1. Linear Discriminant Analysis (LDA)

KNN is one of the most widely used ML algorithms. When a test sample is added to the KNN classifier, the number of nearest neighbors, denoted ask, is first determined (**Figure 2**). This algorithm makes predictions by examining its neighbors. The assumption in the KNN algorithm is that similar objects are close to each other.[19]

Another effective statistical classifier frequently used in small and medium-scale applications is Support Vector Machines (SVM). SVM aims to enhance the separation of examples in a new high-dimensional space by transforming the inputs into this space (**Figure 3**). It groups the data by drawing linear or non-linear curves.[20]

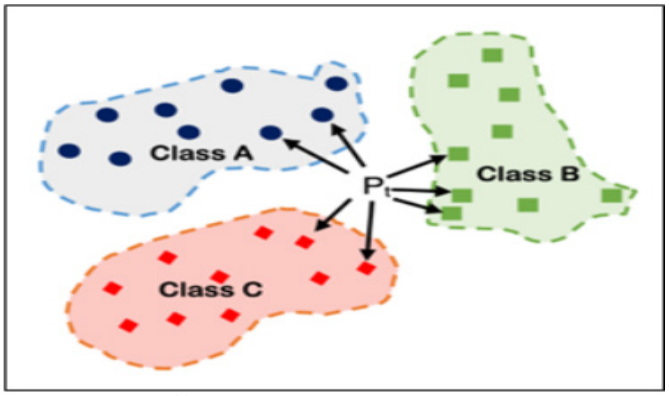

Figure 2. K-Nearest Neighbors (KNN)

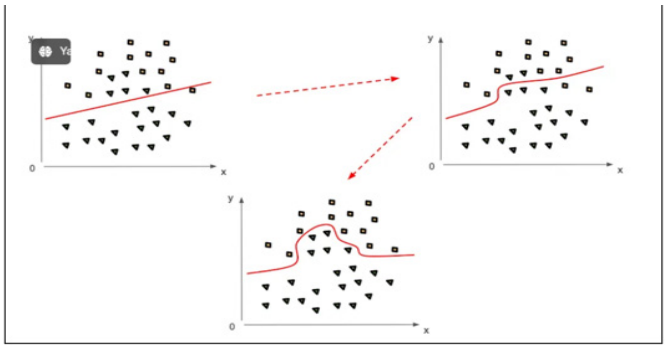

Figure 3. Support Vector Machines (SVM)

Decision trees is a method that has many real-life similarities and impacts a wide range of ML areas, encompassing both classification and regression. A decision tree can visually and comprehensibly present decisions and decision-making processes within the framework of decision analysis (**Figure 4**). As the name suggests, it forms a decision model using a tree-like structure.[21]

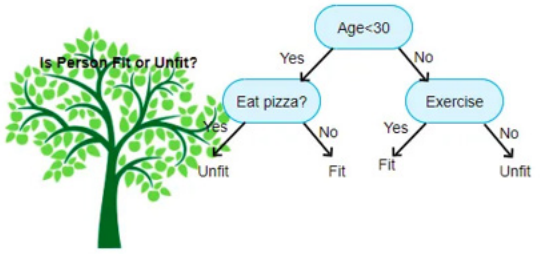

Figure 4. Decision tree

Random Forest, as the name suggests, primarily involves the algorithm creating a random forest (**Figure 5**). There is a direct relationship between the number of trees used in the algorithm and the results obtained. Increasing the number of trees yields more accurate results.[22]

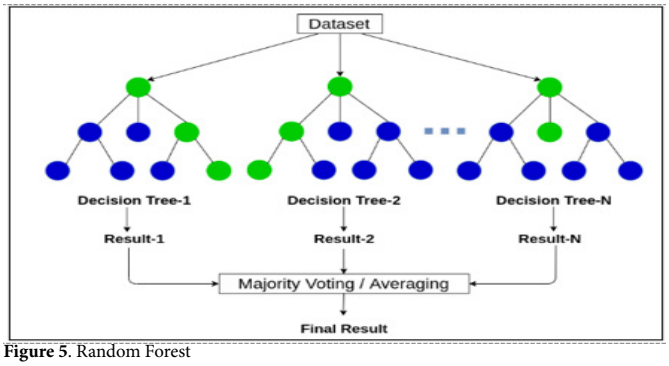

Figure 5. Random Forest

Artificial Neural Networks (ANNs) are a computational technique developed by mimicking the information processing methods of the human brain. ANNs simulate the functioning of biological neurons and the synaptic connections between these cells. Neurons combine in various forms to create networks (**Figure 6**). These networks have the ability to learn, form memories, and discover relationships between data. Similar to biological neural networks, learning in ANNs is achieved through training processes using examples. In other words, the processing of input-output data involves repeatedly adjusting connection weights via the training algorithm until a convergence point is reached. ANNs can be described as structures composed of numerous simple processing units, each dealing with a part of a larger problem. In its simplest form, a processing unit multiplies the input by a set of weights, applies a non-linear transformation, and produces an output value. Artificial neural networks also possess the ability to generalize and work with incomplete data.[23]

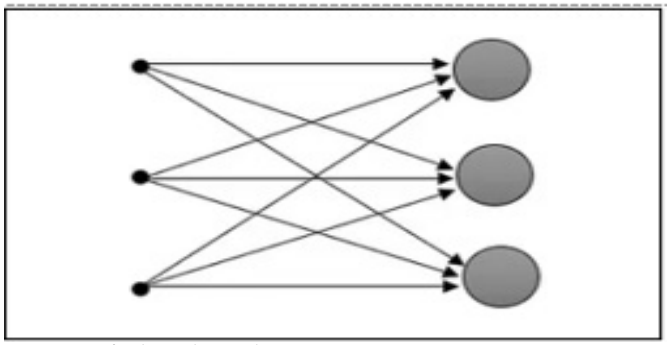

Figure 6. Artificial neural network

STUDIES ON THE USE OF ARTIFICIAL INTELLIGENCE IN AGE ESTIMATION

Hsieh et al.[24] (2007) developed a computer-based bone age estimation system by examining the geometric properties of the carpal bones of the hand. In this system, the bone age of children was categorized using four different classifiers (linear, nearest neighbor, backpropagation neural network, and radial basis function neural network). The study was based on a database of hand radiographs from 65 boys and 444 girls. The proposed normalization area ratio method was found effective in bone age classification, yielding results similar to the Greulich and Pyle atlas (**Figure 7**). The findings indicate that the discriminative power of bone area is high and that the evaluation of carpal bones can be accurately performed with neural networks. The bone age estimation was conducted using four different classifiers: linear classifier, nearest neighbor method, backpropagation neural network, and radial basis function neural network.[24]

Figure 7. Child hand graph example

Koitka et al.[25] (2020) developed a method in their studies that includes a detector network that identifies ossification areas in bone age estimation, along with gender- and region-specific regression networks that estimate age from these areas.

Deshmukh and Khaparde[26] (2022) developed a method based on a region-based convolutional neural network (R-CNN) model by considering the middle phalanx of the 3rd finger, third metacarpal, radius, and ulna regions of the hand (**Figure 8**).

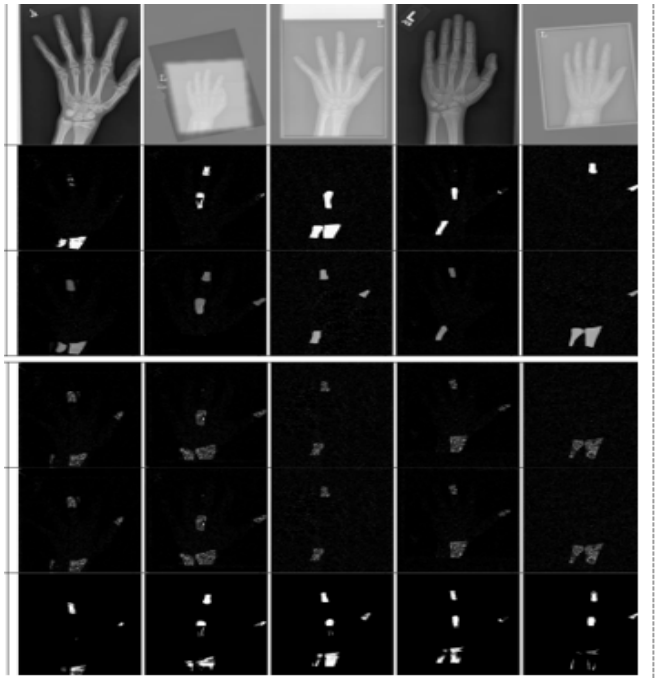

Figure 8. Bones used in Deshmukh and Khaparde's study

In the research by Demirel and Sonuç,[27] a local dataset containing left-hand radiographs of boys and girls aged 1-7 was used, and carpal bones were segmented through edge and contour detectors. The areas and the distal epiphysis region of the radius were loaded into the artificial neural network, and the accuracy rate of the age estimation obtained was determined to be 87%.

In their studies, Mohtarami et al.[28] evaluated the usability of facial angles (glabela and maxilla angles) obtained from tomography scans of a group consisting of 100 men and 100 women, along with data such as the length and width of the piriformis, in age estimation using ML algorithms, and the obtained accuracy rate was found to be 88% (**Figure 9**).

Çiftçi and Seçgin[29] retrospectively examined the foot radiographs of 341 individuals aged 8-65. Parameters such as the maximum width of the calcaneus, body width, maximum length, minimum length, facies articularis cuboidea height, and tuber calcanei width were measured from the radiographs, and participants were divided into three groups: 20-45 years, 46-64 years, and 65 years and older (**Figure 10**). The accuracy rate was determined to be 85%, leading to the conclusion that the calcaneus bone can be evaluated with high accuracy and sensitivity for age estimation.

Ataş and Özdemir[30] conducted a study using panoramic dental radiographs of 1332 individuals aged 8 to 68 to estimate forensic age, and using the InceptionV3 neural network, they achieved 87% accuracy in forensic age estimation. Narin and Yeniçeri[31] examined the hand and wrist radiographs of 388 boys and 387 girls aged 1-9 and calculated the ratio of bone tissue area to total hand and wrist area for each individual,

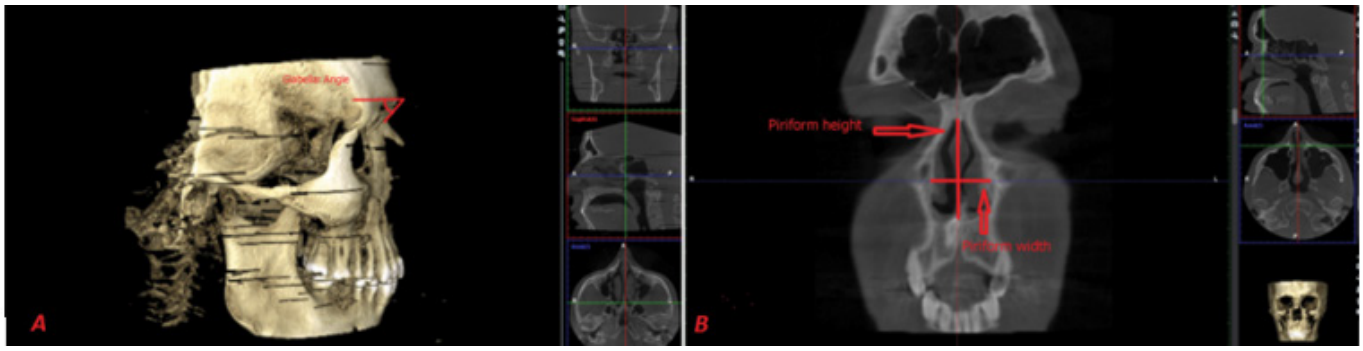

Figure 9. Glabella and piriform measurements used in the study by Mohtarami, Hedjazi and Manouchehri

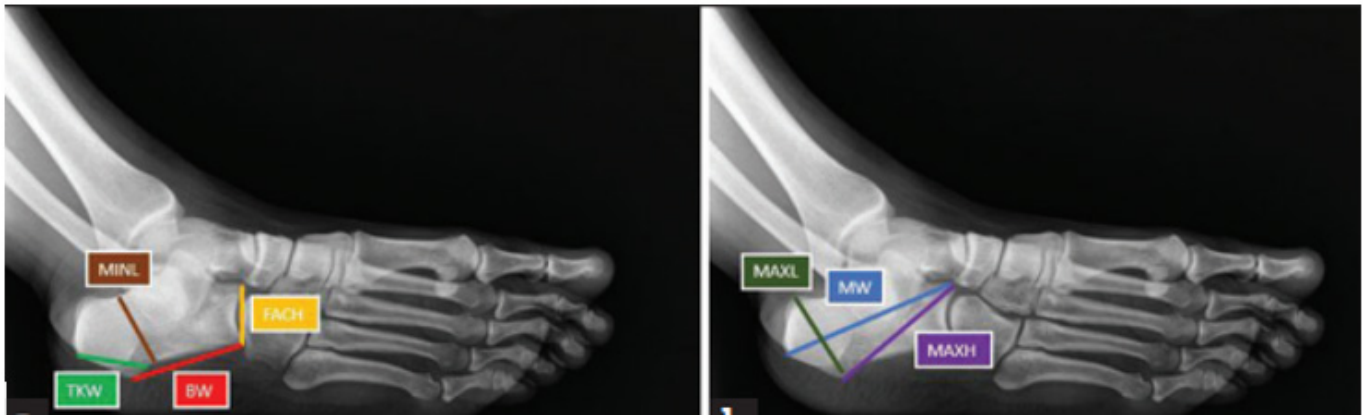

Figure 10. Foot bone parameters used in Çiftçi and Seçgin's study

classifying these data into three-month intervals. These data were accepted as a database, and the test data were compared with this database. Prediction models based on ML were used for bone age estimation, and age estimation was achieved with 95% accuracy using artificial intelligence.

Polat and Çelenk[32] conducted a study aimed at determining reliable, practical, and accurate methods for estimating dental age by examining the volumetric properties of teeth and pulp using three-dimensional images obtained through Cone Beam Computed Tomography.

Chen Fang et al.[33] focused on the use of DNA methylation in forensic genetics for determining chronological age in their research. The study suggested that microRNAs (miRNAs), a group of small non-coding RNAs, show a wide variability with age and could potentially be useful in age estimation. The study involved analyzing the expression profiles of miRNAs obtained from blood samples using large parallel sequencing methods. Age-related miRNAs were identified for age estimation, and seven different machine learning models were used to create age prediction models based on blood stains from individuals aged 20-69 years. The study reported an average error of 5.52 years for males and 7.46 years for females in age estimation.

CONCLUSION

Traditional methods and statistical analyses are frequently used in forensic age estimation; however, errors may occur in these studies due to factors such as data deficiencies, individual differences, and environmental influences, preventing the desired accuracy from being achieved. With the advancement of machine learning, artificial intelligence has become a critical tool in forensic age estimation. The developed algorithms, especially those using biometric data and image processing results, demonstrate that age estimation can be performed with high success rates and accuracy. Furthermore, AI has the potential to provide valuable insights into individuals' health status related to age estimation. These findings highlight the possibilities of AI in health assessment and age estimation.

The use of artificial intelligence in forensic age estimation increases the accuracy of the methods used and enables rapid results. The time-consuming and costly nature of traditional methods makes the application of AI in this field more appealing. To further develop AI applications, it is essential to diversify datasets, continuously update algorithms, and collect diverse data that include different ethnicities, genders, and age groups. This would help eliminate biases in AI systems and adopt a more universal approach. Additionally, attention to the privacy of health data and ethical considerations will enhance the reliability of AI applications.

In conclusion, artificial intelligence and machine learning have the potential to bring significant changes in forensic age estimation. This not only increases the efficiency of forensic systems but also provides more accurate and reliable information about individuals' health conditions.

ETHICAL DECLARATIONS

Referee Evaluation Process

Externally peer-reviewed.

Conflict of Interest Statement

The authors have no conflicts of interest to declare.

Financial Disclosure

The authors declared that this study has received no financial support.

Author Contributions

All of the authors declare that they have all participated in the design, execution, and analysis of the paper, and that they have approved the final version.

REFERENCES

1. Baransel Isır A. Adli hekimlikte yaş tayini. In: Koç S, Can M, eds. Birinci Basamakta Adli Tıp. 2nd ed. İstanbul: İstanbul Tabip Odası Yayınları; 2011: 222-35.
2. Çizmecioğlu FM. Çocukluk çağında kemik yaşı; endokrinolojik yaklaşım. In: Koç S, Can M, eds. 6. Tıp Hukuku Günleri Yaş Tayini-Prof Dr Şemsi Gök Anısına. Adli Tıp Uzmanları Derneği Yayını: 2017;2:80-90.
3. Şener MT, Polat Ş. Adli yaş tahmini yapılan olguların değerlendirilmesi: retrospektif bir çalışma. *KSÜ Tip Fak Der*. 2020;15(2):1-6.
4. Karaturgut UE. Süleyman Demirel Üniversitesi Diş Hekimliği Fakültesine başvuran hastalarda maksilla üzerinde yüz yumuşak doku kalınlık ölçümlerinin değerlendirilmesi. [Doktora tezi]. Isparta: Süleyman Demirel Üniversitesi, Sağlık Bilimleri Enstitüsü; 2017.
5. Orhan M. İnsan daimî dişlerinin konik ışınlı bilgisayarlı tomografi ve periapikal radyografi görüntülerinde pulpa boyutu ve hacminin değerlendirilmesiyle yaş tahmini yapılması. [Diş hekimliği uzmanlık tezi]. Isparta: Süleyman Demirel Üniversitesi, Diş Hekimliği Fakültesi; 2015.
6. Onarici A. Yargı kararları ışığında Türk vergi hukukunda muvazaa ve peçeleme işlemleri. [Yüksek lisans tezi]. Gaziantep: Gaziantep Üniversitesi, Sosyal Bilimler Enstitüsü; 2021.
7. Çelik FE. Funeral transactions of foreigners who die in Turkey. *Milletlerarası Hukuk ve Milletlerarası Özel Hukuk Bülteni*. 2017;37(2):257-93.
8. Kaplan A. 12 yaş ve üstü pediatrik yaş grubunda kemik yaşı tayini için çekilen el bileği grafisinde kullanılan Greulich-Pyle ve Tanner-Whitehouse yöntemlerinin karşılaştırılması. [Tıpta uzmanlık tezi]. İstanbul: İstanbul Üniversitesi, Tıp Fakültesi; 2014.
9. Karabakır B. Adli olguların canlıda yaş tayini açısından incelenmesi. [Doktora tezi]. İstanbul: İstanbul Üniversitesi, Adli Tıp Enstitüsü; 2015.
10. Yüksel A, Tümer AR, Balseven Odabaşı A. Assessment of forensic age and ossification of the medial clavicular epiphysis using computed tomography. *Turkiye Klinikleri J Foren Med*. 2008;5(1):1-5.
11. Tobcu E, Gökalp G. İnce kesitli bilgisayarlı tomografide sakral vertebralar arası füzyon derecesine bakılarak yaş tayini değerlendirilmesi. *Uludağ Tip Derg*. 2021;47(3):341-347.
12. Buran CF. Kafatası bimastoid çapının bilgisayarlı tomografi ile değerlendirilmesinin cinsiyet tayininde kullanılabilirliği. [Tıpta uzmanlık tezi]. İzmir: Dokuz Eylül Üniversitesi, Tıp Fakültesi; 2015.
13. Sezgin N, Ersoy G. Kulak ölçü ve yerleşiminde yaşa bağlı metrik değişimler. *Bulletin Legal Med*. 2020;25(2):106-115.
14. Bayraktar E. Adli yaş tayininin üç boyutlu cone beam bilgisayarlı tomografide diş pulpa kavitesi ile değerlendirilmesi. [Tıpta uzmanlık tezi]. Bursa: Uludağ Üniversitesi, Tıp Fakültesi; 2017.
15. Öztürk AF. Fotoantropometri yöntemi ile sağlıklı çocukların yüzleri üzerindeki referans noktalarından yaş gruplaması ve yaş tahmini [Doktora tezi]. Ankara: Ankara Üniversitesi, Tıp Fakültesi; 2022.
16. Türkoğlu A, Tokdemir M, Sehlikoğlu K, Tunçez FT, Cavlak N, Börk T. Assessing cases of applying for determining the bone age to forensic medicine department of Fırat University between 2010-2015 years. *Turkiye Klinikleri J Foren Med*. 2016;13(1):1-7.
17. Garan A. Diyabetik çocukların adli tıbbi yaş tayini açısından değerlendirilmesi. [Tıpta uzmanlık tezi]. Düzce: Düzce Üniversitesi, Tıp Fakültesi; 2016.
18. Seçmen MZ, Patır S. Narx (doğrusal olmayan otoregresif dışsal girdili) yapay sinir ağları modeli ile otomobil satışı talep tahmini. *Güncel Pazarlama Yaklaşımları ve Araştırmaları Derg*. 2024;5(1):31-47.
19. Peker AA. Akciğer metastazlarında primer tümör kaynağının yapay zekâ algoritmaları ile değerlendirilmesi. [Tıpta uzmanlık tezi]. İstanbul: Bezmialem Vakıf Üniversitesi, Tıp Fakültesi; 2021.
20. Akça MF. Görüş: Nedir bu destek vektör makineleri? (Makine öğrenmesi serisi-2). [Internet]. 2020. Available from: https://medium.com/deep-learning-turkiye/nedir-bu-destek-vekt%C3%B6r-makineleri-makine-%C3%B6%CC%87renmesi-serisi-2-94e576e4223e. Accessed August 22, 2024.
21. Akça MF. Görüş: Karar ağaçları (Makine öğrenmesi serisi-3). [Internet]. 2020. Available from: https://medium.com/deep-learning-turkiye/karar-a%C4%9Fa%C3%A7lar%C4%B1-makine-%C3%B6%C4%9Frenmesi-serisi-3-a03f3ff00ba5. Accessed August 22, 2024.

22. Dündar B. Görüş: Makine öğrenmesi serisi-4 (Machine learning series 4). [Internet]. 2022. Available from: https://medium.com/@beyzadndar/makine-%C3%B6%C4%9Frenmesi-serisi-4-machine-learning-series-4-88c26c599351. Accessed August 21, 2024.
23. Yapay sinir ağları. [Internet]. Available from: https://tr.wikipedia-on-ipfs.org/wiki/Yapay_sinir_a%C4%9Flar%C4%B1. Accessed August 20, 2024.
24. Hsieh CW, Jong TL, Chou YH, Tiu CM. Computerized geometric features of carpal bone for bone age estimation. *Chin Med J*. 2007;120(9):767-770.
25. Koitka S, Kim MS, Qu M, Fischer A, Friedrich CM, Nensa F. Mimicking the radiologists' workflow: estimating pediatric hand bone age with stacked deep neural networks. *Med Image Anal*. 2020;64:101743. doi: 10.1016/j.media.2020.101743
26. Deshmukh S, Khaparde A. Faster region-convolutional neural network oriented feature learning with optimal trained recurrent neural network for bone age assessment for pediatrics. *Biomed Signal Process Control*. 2022;71(12):103016.
27. Demirel O, Sonuç E. Yapay zeka teknikleri kullanılarak kemik yaşı tespiti. *Türkiye Sağlık Enstitüleri Başkanlığı Derg*. 2021;4(3):17-30.
28. Mohtarami SA, Hejaz SA. Determine the age range based on machine-learning methods from skeletal angles of the face (glabella and maxilla angle and length and width of piriformis) in a CT scan. *Int J Med Toxicol Forensic Med*. 2022;12(4):38605.
29. Ciftci R, Secgin Y, Oner Z, Toy S, Oner S. Age estimation using machine learning algorithms with parameters obtained from x-ray images of the calcaneus. *Niger J Clin Pract*. 2024;27(2):209-213.
30. Ataş İ, Özdemir C, Ataş M, Doğan Y. Forensic dental age estimation using modified deep learning neural network. *Balkan J Electr Comput Eng*. 2023;11(4):298-305.
31. Gökçe Narin N, Yeniçeri İÖ, Yüksel G. Estimation of bone age from radiological images with machine learning. *MMJ*. 2021;8(2):119-126.
32. Polat Y, Çelenk SA. Current perspective on novel methods for determınıng dental age in the new generation: a review. *HRU Int J Dent Oral Res*. 2023;3(3):173-177.
33. Fang C, Liu X, Zhao J, et al. Age estimation using bloodstain miRNAs based on massive parallel sequencing and machine learning: a pilot study. *Forensic Sci Int Genet*. 2020;47:102300. doi: 10.1016/j.fsigen.2020.102300